
Masters Theses

Student Theses and Dissertations

1969

Effect of axial mixing in gas absorption

Sundareswaran Parameswaran Iyer

Follow this and additional works at: https://scholarsmine.mst.edu/masters_theses



Part of the [Chemical Engineering Commons](#)

Department:

Recommended Citation

Iyer, Sundareswaran Parameswaran, "Effect of axial mixing in gas absorption" (1969). *Masters Theses*. 7058.

https://scholarsmine.mst.edu/masters_theses/7058

This thesis is brought to you by Scholars' Mine, a service of the Missouri S&T Library and Learning Resources. This work is protected by U. S. Copyright Law. Unauthorized use including reproduction for redistribution requires the permission of the copyright holder. For more information, please contact scholarsmine@mst.edu.

EFFECT OF AXIAL MIXING IN GAS ABSORPTION

2248

By

SUNDARESWARAN PARAMESWARAN IYER - 1944

A

THESIS

submitted to the faculty of

UNIVERSITY OF MISSOURI - ROLLA

in partial fulfillment of the requirements for the

Degree of

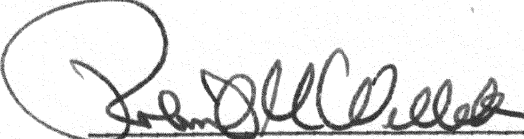
MASTER OF SCIENCE IN CHEMICAL ENGINEERING

Rolla, Missouri

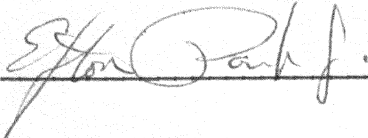
1969

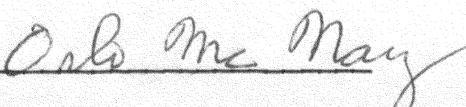
T2319
109 pages
c. 1

Approved by



(advisor)





183304

TABLE OF CONTENTS

	Page
ABSTRACT.....	iv
ACKNOWLEDGEMENT	vi
LIST OF ILLUSTRATIONS	vii
LIST OF TABLES	ix
NOMENCLATURE.....	x
I. INTRODUCTION.....	1
II. PROPOSED MATHEMATICAL MODELS.....	7
A. Case 1. One Parameter System	9
B. Case 2. Two Parameter System.....	9
C. Case 3. Two Parameter System.....	10
D. Case 4. Three Parameter System	11
III. SOLUTION OF THE MATHEMATICAL MODELS	14
A. Derivation of Normal Equations.....	14
1. Case 1. Plug Flow in the Gas Phase and Plug Flow in the Liquid Phase	14
2. Case 3. Plug Flow in the Gas Phase and Axial Mixing in the Liquid Phase ...	16
B. Solution of Normal Equations	19
1. Case 1	19
2. Case 3	22

	Page
IV. RESULTS AND DISCUSSION.....	24
A. One Parameter Model.....	24
B. Two Parameter Model	25
C. Applicability of the Models	26
V. SUMMARY AND CONCLUSION	28
VI. APPENDICES	31
APPENDIX A. Derivation of Boundary Conditions for an Absorption Column	32
APPENDIX B. Equation of Continuity for Homogeneous Flow Systems	38
APPENDIX C. Normal Equation for Case 1.....	41
APPENDIX D. Normal Equations for Case 3.....	44
APPENDIX E. Flow Chart for Case 1.....	52
APPENDIX F. Flow Chart for Case 3.....	66
APPENDIX G. Computer Program for the Plotter....	74
VII. BIBLIOGRAPHY.....	96
VIII. VITA	98

ABSTRACT

The effect of axial mixing in the liquid phase on the performance of a gas-absorption column was studied using the experimental data of Michael Brittan⁽¹⁾ for the carbon dioxide and water system. In this study, piston flow conditions were assumed for the gas phase.

A one-parameter mathematical model, which characterized the flow regimes in both the gas and the liquid phases undergoing plug flow conditions, was first curve fitted for its unknown parameter (i. e. the Number of Transfer Units) by a non-linear regression analysis procedure. The "AAPD" (i. e. the Average Absolute Percentage Deviation between the predicted value of the gas phase concentration and the experimental data) was also computed for each set of data.

An attempt was made to curve-fit a two-parameter mathematical model, which assumed plug flow in the gas phase but axial mixing in the water phase, by a similar non-linear regression analysis procedure. However, in the iterative technique used, the values of the unknown parameters (i. e. , the water phase axial mixing parameter and the number of transfer units) failed to converge. As an alternate to this procedure a graphical method was used to study the effect of the axial mixing parameter on the value of the "AAPD".

The results obtained from the analysis of the two mathematical models were examined. A comparison showed that the "AAPD" computed for both the models were very close; hence, it was concluded that the effect of axial mixing in the water phase, for the nitrogen carbon dioxide-water system

based on the data obtained by Brittan and Woodburn⁽²⁾ has little influence on the gas-absorption column.

ACKNOWLEDGEMENT

A debt of gratitude is due Dr. R. M. Wellek for suggesting, guiding and encouraging this investigation and serving as the research advisor. Sincere appreciation is due Mr. V. K. Mathur for his assistance on the subject, to the Computer Science Center for the computational work carried out on IBM 360 Model and, for plotting the graphs on Calcomp Digital Incremental Plotter, and to Miss Barbara Burbank, for her cooperation in typing this thesis.

This work is dedicated to my mother Bhagirathi, for her invaluable encouragement and endurance, shown during the tennure of my entire education.

S. P. Iyer

LIST OF ILLUSTRATIONS

Figure		Page
I.1	Concentration Profile, for Plug Flow and Axial Mixing Cases, in a Typical Absorption Column.....	3
A.1	Gas and Liquid Flow Regimes at the Bottom of an Absorption Tower.....	33
A.2	Concentration Profile at the Bottom of an Absorption Tower....	33
A.3	Gas and Liquid Flow Regimes at the Top of an Absorption Tower.....	34
A.4	Concentration Profile at the Top of an Absorption Tower.....	34
G.	Effect of Liquid Phase Axial Mixing Parameter on Average Absolute Percentage Deviation, With Number of Transfer Units as the Parameter	
1.	$G = 9.583,$ $L = 9195.00,$ $N_{OX} = 1.09$ to 1.43	78
2.	$G = 9.578,$ $L = 7356.00,$ $N_{OX} = 1.09$ to 1.43	79
3.	$G = 9.575,$ $L = 5517.00,$ $N_{OX} = 1.09$ to 1.43	80
4.	$G = 9.588,$ $L = 3678.00,$ $N_{OX} = 1.09$ to 1.43	81
5.	$G = 7.668,$ $L = 9195.00,$ $N_{OX} = 1.09$ to 1.43	82
6.	$G = 7.677,$ $L = 7356.00,$ $N_{OX} = 1.09$ to 1.43	83
7.	$G = 7.642,$ $L = 5517.00,$ $N_{OX} = 1.09$ to 1.43	84
8.	$G = 7.670,$ $L = 3678.00,$ $N_{OX} = 1.09$ to 1.43	85
9.	$G = 7.661,$ $L = 2298.75,$ $N_{OX} = 0.91$ to 1.25	86

			Page
10.	G = 5.747,	L = 9195.00, N _{ox} = 0.57 to 0.91.....	87
11.	G = 5.747,	L = 7356.00, N _{ox} = 0.75 to 1.09.....	88
12.	G = 5.755,	L = 5517.00, N _{ox} = 0.75 to 1.09.....	89
13.	G = 5.755,	L = 3678.00, N _{ox} = 0.91 to 1.25.....	90
14.	G = 5.749,	L = 2298.75, N _{ox} = 0.91 to 1.25.....	91
15.	G = 3.830,	L = 9195.00, N _{ox} = 0.61 to 0.27.....	92
16.	G = 3.822,	L = 7356.00, N _{ox} = 0.61 to 0.27.....	93
17.	G = 3.827,	L = 5517.00, N _{ox} = 0.57 to 0.91.....	94
18.	G = 3.828,	L = 3678.00, N _{ox} = 0.75 to 1.09.....	95

LIST OF TABLES

Table	Page
I. Data Selected for the Study.....	59
II. Concentration of Carbon Dioxide in Gas Phase, Experimental Against Predicted.....	61
III. Computed Values of One Parameter Model.....	64
IV. Computed Values of Two Parameter Model	73

NOMENCLATURE

- a = Interfacial area between two phases, per unit volume, (sq. ft.)/(cu. ft.)
 A_c = Cross-section area of the column, sq. ft.
 B = L/d , dimensionless, ft./ft.
 c_{x_0} = Initial concentration of the incoming X phase, mole/cu. ft.
 c_{x_0} = $(c_x)_{z=0}$, mole/cu. ft.
 c_{y_L} = Initial concentration of the incoming Y phase, mole/cu. ft.
 c_{y_L} = $(c_y)_{z=L}$, mole/cu. ft.
 d = A representative length, ft.
 E_i = Axial dispersion coefficient of i phase, in the direction of flow, sq. ft./hr.
 F_i = Superficial mass flow rate of i phase, (lb.)/(hr.)(sq. ft.)
 H = Henry's law solubility coefficient, atm./mole fraction.
 H_{oi} = Apparent height of a transfer unit, ft.
 $K_i a$ = Apparent capacity overall mass transfer coefficient based on i phase, (lb. mole)/(hr.)(cu. ft.)(lb. mole/cu. ft.)
 L = Total height of the packing, ft.
 m = Equilibrium distribution coefficient of a transferring component between X and Y phases, dimensionless.
 n = Number of data points along the length of the column.
 N_{oi} = Apparent number of overall transfer units.
 P_i = Axial dispersion group, $(U_i \cdot L)/(E_i)$
 P_T = Total pressure in the column, atm.

- R = Liquid phase axial mixing parameter, $P_y B$.
- U_i = Superficial velocity of the i phase, ft./hr.
- X = Gas phase, (carbon dioxide and nitrogen)
- Y = Liquid phase, (water)
- z = Axial co-ordinate, distance between mean flow (X phase inlet is taken as the original point), ft.

Reduced co-ordinates:

- C_x = c_x/c_{x0} , dimensionless, mole fraction.
- C_y = c_y/c_{y0} , dimensionless, mole fraction.
- Z = z/L , dimensionless, ft./ft.
- C_x^* = Concentration of the solute in the X phase, predicted from the mathematical models, dimensionless, mole fraction.

Greek Letters:

- ϵ_i = Void fraction of i phase, cu. ft./cu. ft.
- $\bar{\epsilon}$ = $(C_{xi} - C_{xi}^*)$, deviation between experimental and predicted gas phase concentration
- ρ_i = Density of i phase, lb. mole/cu. ft.
- λ = $-N_{ox} (1 - \Lambda)$
- Λ = Extraction factor, $(m F_x)/F_y$, dimensionless.
- $\phi(c_i)$ = Volume rate of reaction, lb. mole/(cu. ft.)(hr.)
- $\sigma^2(C_x)$ = Variance on gas phase concentration.
- $\sigma(C_x)$ = Standard deviation on gas phase concentration.
- Δt = Infinitesimal change in time, hr.
- Δz = Infinitesimal change in height, ft.

I. INTRODUCTION

Packed columns are frequently selected as an effective and economical means of interphase contacting for gas-liquid absorption and stripping operations. The usual method of designing an absorption tower involves computing the number of transfer units (NTU) required to bring about a given separation and multiplying by a height factor (HTU) determined from previous experience on the subject. The NTU and the HTU concepts introduced by Colburn^(4, 5) have been applied successfully to absorption towers. In relating the NTU to stream composition Colburn uses a column material balance that inherently assumes a piston flow model for both of the immiscible phases. However, since the concept of plug flow is a hypothetical one, there is some backmixing in all packed towers which invalidates the piston flow assumption inherent in the existing design techniques. Further, Vermeulen⁽¹⁷⁾ and his co-workers have shown that the effect of axial mixing, a deviation from piston flow, may be a significant factor for liquid-liquid extraction systems in packed columns.

The phenomenon of axial mixing arises from the fact that "packets" of fluid do not all move through a packed bed at a constant and uniform velocity. This non-uniform velocity may result from (a) velocity gradients as the fluid flows through the packing and/or (b) eddy motion of the fluid itself. The former is more characteristic of a laminar flow regime; whereas, the latter is probably more characteristic of turbulent flow. McHenry and Wilhelm⁽¹²⁾ report that axial mixing is about six times as great as radial mixing in a packed bed. Axial mixing is, also, the consequence of more complex events such as local trapping, by-passing acceleration and deceleration, than the

stream splitting or 'random walk' mechanism that has served well in explaining radial mixing.

Axial mixing tends to reduce the concentration driving force for interphase mass transfer from that which would exist for piston flow of both phases. This reduction is illustrated in Figure 1, where the concentration profiles for piston flow are represented by the dotted lines and the solid lines represent a typical axial mixing case⁽¹³⁾. Note that there is a discontinuity at the points where the countercurrent streams enter the column where axial mixing is present. (See appendix A). Attempts have been made recently to obtain "true" mass transfer coefficients by measuring concentration distributions within a column. This approach should be more accurate than the alternative of using a logarithmic mean driving force computed only from the end concentrations of the incoming and outgoing streams. In most of the reactor designs, axial diffusion is neglected because axial gradients are often not steep. This omission of axial diffusion may, in some cases be an unsafe assumption as even a small gradient multiplied by a large coefficient in a differential equation can lead to an important element in the solution of the equations.

Ogburn⁽¹⁵⁾ in his studies has indicated that during the hydrogenation of ethylene in a fixed bed of catalyst with an isothermal wall, experimentally determined axial temperature profiles showed several departures from those calculated with all major effects except axial diffusion taken into account. The initial temperature gradient was not as steep as the predicted gradient. The measured peak temperature did not reach the calculated peak; the temperature downstream of the peak fell more rapidly than was anticipated

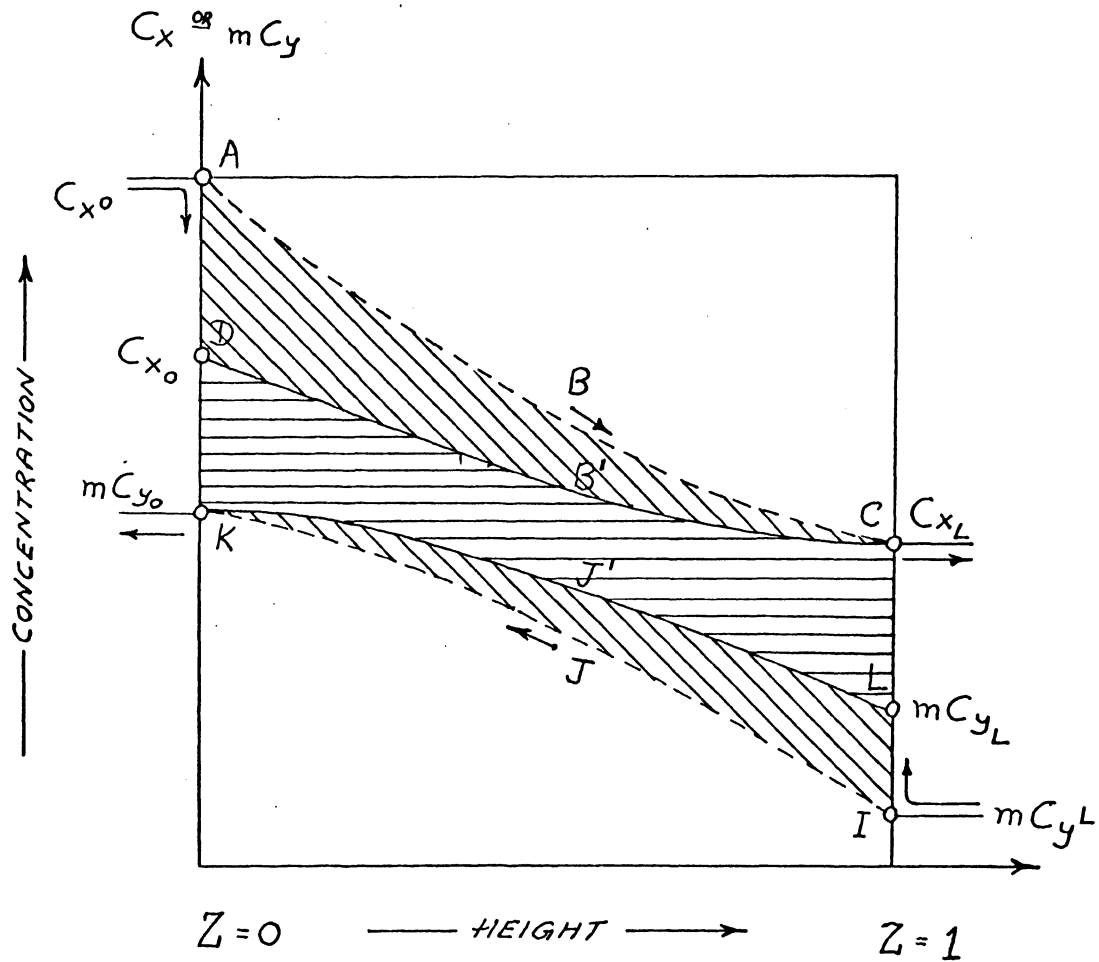


Figure I.1 Concentration Profile, for Plug Flow and Axial Mixing Cases, in a Typical Absorption Column.

Curve IJK = Apparent distribution of carbon dioxide in liquid phase assuming piston flow.

Curve ILJ'K = Actual distribution of carbon dioxide in liquid phase.

Curve ABC = Apparent distribution of carbon dioxide in gas phase assuming piston flow.

Curve ADB'C = Actual distribution of carbon dioxide in gas phase.

from calculations. All three effects point to the presence of an important heat leak away from the equipment from the temperature peak and hence possibly to axial mixing.

Brittan and Woodburn⁽²⁾ studied the absorption of carbon dioxide from mixtures with nitrogen by countercurrent contact with water in an experimental packed tower consisting of a single 3-5/8 inch i.d. glass section, with 1/2-inch raschig rings as the packings, packed to an overall height of 34.75 inches. In the 110 experimental runs conducted, they varied the gas rate from 3.5 lb/(hr)(sq. ft.) to 9.5 lb/(hr)(sq. ft.) and the liquid rate from 2,500 lb/(hr)(sq. ft.) to 9,500 lb/(hr)(sq. ft.). Radial and axial gas concentration profiles were determined from measurements made within the packing. Substantial gas phase channeling was observed. Characterizing the gas flow regime by both piston flow and axial diffusion models yielded mass transfer values and computed axial gas concentration profiles. In both the models, liquid flow regime was characterized by plug flow. The differences between the gas phase compositions predicted by the two models (solved by the Runge-Kutta method of stepwise integration procedure) allowed Brittan to assess the influence of axial dispersion and the applicability of the axial diffusion model.

Owing to the spread of fluid element residence time prevailing in an absorption tower, the resulting longitudinal dispersion will in some measure have an adverse influence on the performance. The magnitude of this effect has not yet been determined, however. For carbon dioxide absorbers, in particular, it has been speculated that the wide discrepancy between the actual industrial scale performance and that predicted from standard mass transfer

correlations^(9, 14, 16) is due to axial dispersion of the gas phase⁽²⁾. In two-phase operation of this nature, substantial gas phase mixing will be induced by the countercurrent liquid flow, particularly at the high water rate necessary to achieve satisfactory absorption of relatively insoluble gas such as carbon dioxide.

The purpose of this investigation is to consider the effect of axial dispersion in the water phase and to determine whether this axial mixing contribution is an important factor in the gas absorption column design for the carbon dioxide-water system. Hoffman⁽⁸⁾ and Levenspiel and Bischoff⁽¹⁰⁾ have postulated a number of mathematical models to describe the mixing characteristics prevailing in continuous flow columns. The mathematical models developed by Miyauchi⁽¹³⁾ have been discussed and treated in this work to analyse the effects of liquid mixing for the carbon dioxide water system. To achieve a given separation, more transfer units and hence, a longer column is required for the axial mixing case owing to the reduced driving force. Likewise, for a given column under the conditions of axial mixing, HUT's reported on the basis of the Colburn equations are higher than the true HTU's that would be calculated from the actual mass transfer coefficients. By making use of the experimental data of the gas phase concentration at various heights along the length of the column, the two mathematical models are solved for the parameters in them. The deviation produced with these computed values of the parameters in predicting the gas phase concentrations along the length of the column from those gas phase concentrations experimentally determined should be a minimum. The solution of the mathematical model for the case

of plug flow in the gas phase and axial mixing in the liquid phase is compared with that for the case of plug flow in both the gas and the liquid phases, in fitting the mathematical model to the experimental curve. Depending upon the mathematical model which gives a better fit to the experimental curve, it may be possible to predict the effect of axial mixing in the liquid phase on the performance of the column.

The one-parameter mathematical model, suited for the plug flow conditions in the gas and the liquid phases (for the experimental data of Brittan) is curve fitted in this work, by the method of least square regression analysis; the value of the parameter N_{ox} (Number of Transfer Units) in the mathematical model that gives the best fit to the experimental curve is designated as the mass transfer parameter characteristic of the experimental system. The two parameter mathematical model which takes into consideration axial dispersion in the liquid phase and plug flow in the gas phase will be curve fitted in this study to the experimental data of Brittan by the method of least squares. Also, the extent to which the value of the gas phase concentration predicted from the mathematical model for the two parameter system deviates from that experimentally determined by changing the value of the axial mixing parameter R in the mathematical model (for the case of plug flow in the gas phase and axial mixing in the liquid phase) will be visually elucidated by plotting the graphs of the axial mixing parameter R against the average deviation produced in absolute terms using N_{ox} as the parameter.

II. PROPOSED MATHEMATICAL MODELS

In gas absorption column design, the values of the design parameters; namely, the overall mass transfer coefficient, the height of a transfer unit, the number of transfer units, etc., are computed from the mass transfer correlations which were evaluated by assuming piston flow conditions in the gas and liquid phases. Investigations by various workers, (1, 12, 15, 17), in the field of gas absorption and those related to it, show that the difference between the industrial scale performance and that predicted from the available mass transfer correlations may be due to the adverse effect caused by the axial mixing of the gas and the liquid phases during their flow through the column. In this chapter, an analysis of the mass transfer relations between the gas and the liquid phases, along the length of the column, is presented. This analysis takes into consideration the axial mixing in both the gas and the liquid phases which occur during their traverse across the packings in the absorption columns. The mathematical models and their respective boundary conditions for the different cases corresponding to the presence and/or absence of axial mixing in the gas and/or the liquid phases, also, have been presented.

For one-dimensional counter-current two phase mass transfer processes Danskohler's⁽⁷⁾ equation of continuity for homogeneous continuous flow systems (see appendix B) may be modified and rearranged into a dimensionless form as follows:

$$\frac{d^2 C_x}{dz^2} - \frac{P_x B}{dZ} \frac{dC_x}{dZ} - N_{ox} \frac{P_x B}{dZ} (C_x - mC_y) = 0 \quad (2.1)$$

$$\frac{d^2 C_y}{dZ^2} + P_{yB} \frac{dC_y}{dZ} + N_{oy} P_{yB} (C_x - mC_y) = 0 \quad (2.2)$$

The dimensionless boundary conditions as shown in appendix A are

$$\text{a) } Z = 0, \quad \text{i) } -\left(\frac{dC_x}{dZ}\right) = P_{xB} (1 - C_x) \quad (2.3)$$

$$\text{ii) } -\left(\frac{dC_y}{dZ}\right) = 0 \quad (2.4)$$

$$\text{b) } Z = 1, \quad \text{i) } -\left(\frac{dC_x}{dZ}\right) = 0 \quad (2.5)$$

$$\text{ii) } -\left(\frac{dC_y}{dZ}\right) = P_{yB} (C_{y1} - C_y) \quad (2.6)$$

In the mathematical models shown above, P_{xB} is the parameter for axial mixing in the gas phase, and P_{yB} is the parameter for axial mixing in the liquid phase. The parameters P_{xB} and P_{yB} are inversely proportional to the eddy diffusivities in the gas and the liquid phases, respectively; $P_{xB} = \frac{U_x L}{E_x}$

and $P_{yB} = \frac{U_y L}{E_y}$, where L is the effective height of the packing, E_x and E_y are the eddy diffusivities in the X and Y phases respectively, $U_x = \frac{F_x}{\epsilon_x}$, and $U_y = \frac{F_y}{\epsilon_y}$, where F_x and F_y are the superficial mass flow rate of the X and the Y phases, respectively. $N_{ox} = \frac{K_x a L}{F_x}$, and $N_{oy} = \frac{K_y a L}{F_y}$, where K_x is the

overall mass transfer coefficient relative to the phase X, and a is the interfacial area per unit volume.

Depending upon the presence and/or absence of the eddy diffusivities E_x and E_y in the individual phases, four different sets of mathematical models are derived from the equations (2.1) and (2.2). The various differential

equations and the boundary conditions which describe the various models are given as follows:

A. Case 1: (One Parameter System)

Conditions of plug flow in the gas and the liquid phases are assumed, i.e. the eddy diffusivities $E_x \rightarrow 0$ and $E_y \rightarrow 0$, so that the axial mixing parameters $P_x B \rightarrow \infty$ and $P_y B \rightarrow \infty$, therefore, from equations (2.1) and (2.2)

$$\frac{dC_x}{dZ} + N_{ox} (C_x - mC_y) = 0 \quad (2.7)$$

and

$$\frac{dC_y}{dZ} + N_{oy} (C_x - mC_y) = 0 \quad (2.8)$$

The necessary boundary conditions are

$$a) \quad Z = 0, \quad i) \quad C_x = 1 \quad (2.3a)$$

$$ii) \quad -\left(\frac{dC_y}{dZ}\right) = 0 \quad (2.4)$$

$$b) \quad Z = 1, \quad i) \quad -\left(\frac{dC_x}{dZ}\right) = 0 \quad (2.5)$$

$$ii) \quad C_{y_1} = C_y \quad (2.6a)$$

B. Case 2: (Two Parameter System)

Conditions of axial mixing in the gas phase and plug flow in the liquid phase are assumed, i.e. the eddy diffusivities E_x is finite and $E_y \rightarrow 0$, so that $P_x B$ is finite and $P_y B \rightarrow \infty$; Therefore, equations (2.1) and (2.2) are reduced to

$$\frac{d^2 C_x}{dZ^2} - P_x B \frac{dC_x}{dZ} - N_{ox} P_x B (C_x - mC_y) = 0 \quad (2.1)$$

and

$$\frac{dC_y}{dZ} + N_{oy} (C_x - mC_y) = 0 \quad (2.8)$$

and the associated boundary conditions are,

$$\text{a) } Z = 0, \quad \text{i) } -\left(\frac{dC_x}{dZ}\right) = P_x B (1 - C_x) \quad (2.3)$$

$$\text{ii) } -\left(\frac{dC_y}{dZ}\right) = 0 \quad (2.4)$$

$$\text{b) } Z = 1, \quad \text{i) } -\left(\frac{dC_x}{dZ}\right) = 0 \quad (2.5)$$

$$\text{ii) } C_{y_1} = C_y \quad (2.6a)$$

C. Case 3: (Two Parameter System)

This case is the reverse of Case 2. Here the conditions assumed are plug flow in the gas phase and axial mixing in the liquid phase, i.e. the eddy diffusivities are given by $E_x \rightarrow 0$. E_y is finite so that the axial mixing parameters reduce to $P_x B \rightarrow \infty$, and $P_y B$ is finite. Therefore, from equations (2.1) and (2.2)

$$\frac{dC_x}{dZ} + N_{ox} (C_x - mC_y) = 0 \quad (2.7)$$

and

$$\frac{d^2 C_y}{dZ^2} + P_y B \frac{dC_y}{dZ} + N_{oy} P_y B (C_x - mC_y) = 0 \quad (2.2)$$

where the necessary and sufficient boundary conditions are

$$\text{a) } Z = 0, \quad \text{i) } C_x = 1 \quad (2.3a)$$

$$\text{ii) } -\left(\frac{dC_y}{dZ}\right) = 0 \quad (2.4)$$

$$\text{b) } Z = 1, \quad \text{i) } -\left(\frac{dC_x}{dZ}\right) = 0 \quad (2.5)$$

$$\text{ii) } -\left(\frac{dC_y}{dZ}\right) = P_y B (C_{y_1} - C_y) \quad (2.6)$$

D. Case 4: (Three Parameter System)

This case represents the extreme case where conditions of axial mixing is assumed in both the gas and the liquid phases, i. e. the eddy diffusivities E_x and E_y in the gas and the liquid phases, respectively, are finite which means that the axial parameters $P_x B$ and $P_y B$ in the respective phases are finite. This case is represented by equations (2.1) and (2.2), and the boundary conditions incorporated herein are as given by equations (2.3), (2.4), (2.5), and (2.6).

Brittan has analysed Case 2 and has compared the results with those obtained from Case 1; he has employed a numerical integration method for analysing the aforesaid cases and thereby has predicted the effect of axial mixing in the gas phase on the performance of the absorption column for the carbon dioxide-water system. In this study, Case 3 is analysed, and the results are compared with those computed for Case 1; a non-linear regression analysis method and a graphical technique are used to predict the effect of axial mixing in the liquid phase on the performance of the column. In the following section, the foresaid methods are employed for computing the values of the axial mixing parameter, $P_y B$, and the number of transfer units, N_{ox} in the mathematical models represented by the Cases 1 and 3.

Depending upon the definition of the concentration driving force there should be three kinds of HTU (i.e. height of transfer unit):

i. "True" values:

By the original definition of HTU⁽³⁾, "true" HTU is the ratio of volumetric flow rates across a unit cross-section to the true over-all coefficient of mass transfer.

$$H_{oxT} = \frac{F_x}{K_x a} \quad (2.9)$$

Likewise, the true number of overall transfer units (NTU) is

$$N_{oxT} = \frac{K_x a L}{F_x} \quad (2.10)$$

ii. "Measured" values:

When an absorber behaves in the same manner as the proposed model, the actual concentration distribution for the X phase in the absorber is given by curve ADB'C and for the Y phase by curve ILJ'K in Figure 1. These two curves can be obtained by measuring the concentration distribution in the absorber.

$$N_{oxM} = \int_{C_{xo}}^{C_{xl}} \frac{dC_x}{C_x - mC_y} \quad (2.11)$$

and from this definition of NTU, an apparent HTU is derived as;

$$H_{oxM} = \frac{L}{N_{oxM}} \quad (2.12)$$

iii. "Piston Flow" values:

Another apparent NTU is defined in terms of the logarithmic-mean driving force computed from the exterior incoming and outgoing concentrations at both ends of the absorber:

$$N_{oxP} = \int_{1.0}^{C_{x1}} \frac{dC_x}{C_{xP} - mC_y} \quad (2.13)$$

Integration of the right-hand side of this equation (2.13) gives equations (3.1) and (3.2) for $\Lambda \neq 1$.

The corresponding apparent HTU is defined as

$$H_{oxP} = \frac{L}{N_{oxP}} \quad (2.14)$$

H_{oiM} and H_{oiP} should include the effect of longitudinal dispersion of the transferring material. In general one will find

$$H_{oiP} \geq H_{oiM} \geq H_{oiT}$$

$$N_{oiP} \leq N_{oiM} \leq N_{oiT}$$

Relations between H_{oxT} , H_{oxM} and H_{oxP} have been discussed elsewhere⁽¹³⁾.

III. SOLUTION OF THE MATHEMATICAL MODELS

The mathematical models developed in the preceding section for the conditions of plug flow in both the gas and the liquid phases, represented by case 1 and for the conditions of plug flow in the gas phase but axial mixing in the liquid phase represented by case 3 are treated in this section; the normal equations are derived from the respective differential equations (2.7), (2.8), and (2.7), (2.2) for the two cases and are then solved for the parameters N_{ox} and R & N_{ox} by making use of the IBM 360 Computer. Also, a deviation between the values of the gas phase concentration predicted by the computed parameters and the values experimentally determined is calculated. Further a variance on the parameter N_{ox} , and on the concentration of carbon dioxide in the gas phase c_x , is also shown here:

A. Derivation of Normal Equations:

1. Case 1:

Conditions of plug flow in the gas phase and in the liquid phase are prevalent in this case. The differential equations describing the subject case are,

$$\frac{dC_x}{dZ} + N_{ox} (C_x - mC_y) = 0 \quad (2.7)$$

and

$$\frac{dC_y}{dZ} + N_{oy} (C_x - mC_y) = 0 \quad (2.8)$$

and the boundary conditions are,

$$\text{a) } Z = 0, \quad \text{i) } C_x = 1 \quad (2.3a)$$

$$\text{ii) } -\left(\frac{dC_y}{dZ}\right) = 0 \quad (2.4)$$

$$\text{b) } Z = 1 \quad \text{i) } -\left(\frac{dC_x}{dZ}\right) = 0 \quad (2.5)$$

$$\text{ii) } C_{y_1} = C_y \quad (2.6a)$$

The solutions of the above equations given elsewhere⁽¹³⁾ are as follows:

$$\frac{C_x - mC_{y_1}}{1 - mC_{y_1}} = \frac{e^{\lambda Z} - \Lambda e^{\lambda}}{1 - \Lambda e^{\lambda}} \quad (3.1)$$

and

$$\frac{m(C_y - mC_{y_1})}{1 - mC_{y_1}} = \frac{(e^{\lambda Z} - e^{\lambda})\Lambda}{1 - \Lambda e^{\lambda}} \quad (3.2)$$

Since the concentration in the available nitrogen-carbon dioxide-water experimental data are in the gas phase, equation (3.1) is used as the mathematical model for evaluating the value of the parameter N_{ox} . The carbon dioxide present in the inlet water at the top of the column is negligible, and $C_{y_1} = 0$; hence equation (3.1) reduces to

$$C_x^* = \frac{e^{\lambda Z} - \Lambda e^{\lambda}}{1 - \Lambda e^{\lambda}} \quad (3.3)$$

where

$$\Lambda = m \frac{F_x}{F_y} \quad (3.4)$$

$$\lambda = -N_{\text{ox}} (1 - \Lambda) \quad (3.5)$$

and

C_x^* is predicted value of gas phase concentration.

The mathematical model represented by the equation (3.3) is curve-fitted by a non-linear least square technique for the parameter λ and hence N_{ox} . The "normal equation" as derived by the least square procedure in appendix C is given as follows:

$$\sum_{i=1}^n C_{xi} \left[\frac{Z_i e^{\lambda_0 Z_i} (1 - \Lambda e^{\lambda_0}) + \Lambda e^{\lambda_0} (e^{\lambda_0 Z_i} - 1)}{(1 - \Lambda e^{\lambda_0})^2} \right]$$

$$-\sum_{i=1}^n \left[\frac{e^{\lambda_0 Z_i} - \Lambda e^{\lambda_0}}{1 - \Lambda e^{\lambda_0}} \right] \left[\frac{Z_i e^{\lambda_0 Z_i} (1 - \Lambda e^{\lambda_0}) + \Lambda e^{\lambda_0} (e^{\lambda_0 Z_i} - 1)}{(1 - \Lambda e^{\lambda_0})^2} \right]$$

$$= \sum_{i=1}^n \left[\frac{Z_i e^{\lambda_0 Z_i} (1 - \Lambda e^{\lambda_0}) + \Lambda e^{\lambda_0} (e^{\lambda_0 Z_i} - 1)}{(1 - \Lambda e^{\lambda_0})^2} \right]^2 (\lambda - \lambda_0) \quad (3.6)$$

where λ_0 is the starting value of λ , in the foreshown normal equation, assumed such that the iterated values of λ converges within an allowable error; the error value allowed in this study is of the order of 10^{-8} . By solving for the converged value of λ , it is possible to compute the value of the parameter N_{ox} . A computer program for solving the above shown normal equation is discussed in the next section.

2. Case 3:

Conditions of plug flow in the gas phase but axial mixing in the liquid phase are prevalent in this case. The differential equations for this case are,

$$\frac{dC_x}{dZ} + N_{ox} (C_x - mC_y) = 0 \quad (2.7)$$

and

$$\frac{d^2 C_y}{dZ^2} + P_y B \frac{dC_y}{dZ} + N_{oy} P_y B (C_x - mC_y) = 0 \quad (2.2)$$

and the associated boundary conditions are,

$$a) \quad Z = 0, \quad i) \quad C_x = 1 \quad (2.3a)$$

$$ii) \quad -\left(\frac{dC_y}{dZ}\right) = 0 \quad (2.4)$$

$$b) \quad Z = 1, \quad i) \quad -\left(\frac{dC_x}{dZ}\right) = 0 \quad (2.5)$$

$$ii) \quad -\left(\frac{dC_y}{dZ}\right) = P_x B (C_{y_1} - C_y 1) \quad (2.6)$$

The above basic differential equations are combined to give,

$$\frac{d^3 C_x}{dZ^3} + h \frac{d^2 C_x}{dZ^2} + k \frac{dC_x}{dZ} = 0 \quad (3.7)$$

The solution of the above equation given elsewhere⁽¹³⁾ for the value of $\Lambda \neq 1$ is shown below:

$$\frac{C_x - mC_y 1}{1 - mC_y 1} = H_1 e^{\lambda_1 Z} + H_2 e^{\lambda_2 Z} + H_3 e^{\lambda_3 Z} \quad (3.8)$$

and

$$\frac{m(C_y - mC_y 1)}{1 - mC_y 1} = h_1 H_1 e^{\lambda_1 Z} + h_2 H_2 e^{\lambda_2 Z} + h_3 H_3 e^{\lambda_3 Z} \quad (3.8a)$$

where as shown in appendix D

$$H_1 = \frac{DH_1}{DH} \quad (D.7a)$$

$$H_2 = \frac{DH_2}{DH} \quad (D.7b)$$

$$H_3 = \frac{DH_3}{DH} \quad (D.7c)$$

$$DH = DH_1 + (h_3\lambda_3 - h_2\lambda_2) \quad (D.15)$$

$$DH_1 = \begin{vmatrix} h_2\lambda_2 & h_3\lambda_3 \\ (1 + \frac{\lambda_2}{P_y B}) e^{\lambda_2 Z} h_2 & (1 + \frac{\lambda_3}{P_y B}) e^{\lambda_3 Z} h_3 \end{vmatrix} \quad (D.9a)$$

$$DH_2 = + h_3\lambda_3 \quad (D.9b)$$

$$DH_3 = - h_2\lambda_2 \quad (D.9c)$$

$$h_1 = 1 + \lambda_1 N_{ox} \quad (D.17a)$$

$$h_2 = 1 + \lambda_2 N_{ox} \quad (D.17b)$$

$$h_3 = 1 + \lambda_3 N_{ox} \quad (D.17c)$$

$$\lambda_1 = 0 \quad (D.11a)$$

$$\lambda_2 = -\left(\frac{h}{2}\right) + \sqrt{\left(\frac{h}{2}\right)^2 - k} \quad (D.11b)$$

$$\lambda_3 = -\left(\frac{h}{2}\right) - \sqrt{\left(\frac{h}{2}\right)^2 - k} \quad (D.11c)$$

$$h = N_{ox} + P_y B \quad (D.12a)$$

and

$$k = N_{ox} P_y B (1 - \Lambda) \quad (D.12b)$$

Similar to case 1, equation (3.8) is used as the mathematical model with $C_y = 0$.

Hence equation (3.8) reduces to

$$C_x^* = H_1 e^{\lambda_1 Z} + H_2 e^{\lambda_2 Z} + H_3 e^{\lambda_3 Z} \quad (3.9)$$

The above mathematical model was curve fitted for the parameter N_{ox} and the parameter $P_y B$. In the computer programs, the parameter N_{ox} will be denoted as 'X', and the parameter $P_y B$ will be denoted as 'R'.

The normal equations as derived in appendix D are as follows:

$$\begin{aligned} & \sum_{i=1}^n C_{xi} \left[\frac{dC_{xi}^*}{dX} \right]_{Xo} - \sum_{i=1}^n C_{xo}^* \left[\frac{dC_{xi}^*}{dX} \right]_{Xo} + \sum_{i=1}^n \left[\frac{dC_{xi}^*}{dX} \right]_{Xo}^2 \cdot Xo + \sum_{i=1}^n \left[\frac{dC_{xi}^*}{dX} \right]_{Xo} \left[\frac{dC_{xi}^*}{dR} \right]_{Ro} \cdot Ro \\ & = \sum_{i=1}^n \left[\frac{dC_{xi}^*}{dX} \right]_{Xo}^2 \cdot X + \sum_{i=1}^n \left[\frac{dC_{xi}^*}{dX} \right]_{Xo} \left[\frac{dC_{xi}^*}{dR} \right]_{Ro} \cdot R \end{aligned} \quad (3.10)$$

and

$$\begin{aligned} & \sum_{i=1}^n C_{xi} \left[\frac{dC_{xi}^*}{dR} \right]_{Ro} - \sum_{i=1}^n C_{xo}^* \left[\frac{dC_{xi}^*}{dR} \right]_{Ro} + \sum_{i=1}^n \left[\frac{dC_{xi}^*}{dX} \right]_{Xo} \left[\frac{dC_{xi}^*}{dR} \right]_{Ro} \cdot Xo \\ & + \sum_{i=1}^n \left[\frac{dC_{xi}^*}{dR} \right]_{Ro}^2 \cdot Ro = \sum_{i=1}^n \left[\frac{dC_{xi}^*}{dX} \right]_{Xo} \left[\frac{dC_{xi}^*}{dR} \right]_{Ro} \cdot X + \sum_{i=1}^n \left[\frac{dC_{xi}^*}{dR} \right]_{Ro}^2 \cdot R \end{aligned} \quad (3.11)$$

where Xo and Ro are the starting values of the parameters X (i.e. N_{ox}) and R (i.e. $P_y B$) assumed, in the above normal equation, such that the iterated values of X and R converge as the process of iteration is continued.

B. Solution of the Normal Equations:

The normal equations, as derived in the preceding section for the case of plug flow in both the gas and the liquid phases and for the case of plug flow in the gas phase and axial mixing in the liquid phase, are solved here for their unknown parameters N_{ox} (for case 1) and the parameters N_{ox} and R (for case 3), respectively.

1. Case 1: (Plug flow in both the gas and the liquid phases)

The normal equation represented by the equation (3.6) is solved for the parameter λ by an iterative technique. (See appendix E.) λ is given by the

following equations: $\lambda = -N_{ox} (1 - \Lambda)$, where $\Lambda = m\left(\frac{F_x}{F_y}\right)$. From the iterated value of λ , the number of transfer units N_{ox} is calculated.

(i) Calculation of Average Absolute Percentage Deviation:

AAPD is a form of representing the deviation between the predicted value of the gas phase concentration and the experimental data. By substituting the iterated value of the parameter λ in the mathematical model, equation (3.3), the gas phase concentration C_{xi}^* is predicted at the point 'i' along the length of the column. This value of C_{xi}^* is compared with the experimentally determined gas phase concentration C_{xi} , and their absolute percentage difference divided by the experimental value, C_{xi} is summed up for all the 'n' number of data points along the length of the column. The Average Absolute Percentage Deviation is given by;

$$AAPD = \frac{100}{n} \sum_{i=1}^n \left[\left| \frac{C_{xi} - C_{xi}^*}{C_{xi}} \right| \right] \quad (3.12)$$

The AAPD gives a measure as to how close a given mathematical model, with its computed parameters, fits the experimental curve--the lower the AAPD, the better the fit.

(ii) The "Variance" on gas phase concentration: $\sigma_{(cx)}^2$

An estimate of the probability that the predicted value of the gas phase concentration differs from the experimentally measured value is obtained in terms of 'Variance' or alternatively, as the 'Standard Deviation' as follows:

$$\text{Sample Variance} = \sigma_{(cx)}^2 = \frac{1}{D.F} \sum_{i=1}^n (c_{xi} - c_{xi}^*)^2 \quad (3.13)$$

$$\text{Where D.F. (Degree of Freedom) = } n - m \quad (3.13a)$$

n = total number of data points

m = total number of parameters to be determined.

The sample variance is simply the mean square deviation of the 'n' predicted values from the experimental values. In this definition, positive and negative fluctuations between the predicted and experimental values do not 'cancel' one another.

The standard deviation is given by the following:

$$\sigma_{(cx)} = \text{sample standard deviation} = \sigma_{(cx)}^2 \quad (3.14)$$

This value of the variance becomes more reliable as more experimental data are obtained. The true precision of the procedure of prediction of the gas phase concentration by the mathematical model is indicated by the value of variance calculated from a very large amount of data.

(iii) The "Variance" on the Number of Transfer Units: $\sigma_{(N_{ox})}^2$

The value of λ and hence N_{ox} as calculated from the mathematical model, equation (3.3), is subject to error. This error is a direct consequence of the error in the measured values of C_x . Estimates of the error variance of λ are given by the expression

$$\sigma_{(\lambda)}^2 = \sum_{i=1}^n \left[\frac{\sigma_{(c_{xi})}^2}{\left[\frac{\partial \bar{C}_{xi}^*}{\partial \lambda} \right]^2} \right] \quad (3.15)$$

$$= \left(\frac{1}{D.F} \right) \sum_{i=1}^n \frac{(c_{xi} - \bar{c}_{xi}^*)^2}{\left[\frac{Z_i e^{\lambda Z_i} (1 - \Lambda e^{\lambda}) + \Lambda e^{\lambda} (e^{\lambda Z_i} - 1)}{(1 - \Lambda e^{\lambda})^2} \right]^2} \quad (3.16)$$

The sample standard deviation on λ is given by

$$\sigma(\lambda) = \sqrt{\frac{\sigma^2}{\lambda}} \quad (3.17)$$

The sample standard deviation on N_{ox} is given by

$$\sigma(N_{ox}) = \frac{\sigma(\lambda)}{(\Lambda - 1)} \quad (3.18)$$

$$\text{where } \Lambda = m \frac{F_x}{F_y} \quad (3.4)$$

A computer program was written (See appendix E) for calculating the following quantities:

The number of transfer units N_{ox} ; to predict the value of the gas phase concentration, C_{xi}^* , along the length of the column, in comparison with the experimental data C_{xi} ; the average absolute percentage deviation, between the predicted and the experimental values of the gas phase concentration, AAPD; the variance and the standard deviation, on c_x , $\sigma^2_{(cx)}$ and $\sigma_{(cx)}$; the standard deviation, on N_{ox} , $\sigma(N_{ox})$.

The above values and results for all the 110 runs are tabulated and kept elsewhere⁽¹⁸⁾.

2. Case 3: (Plug flow in the gas phase and axial mixing in the liquid phase)

The normal equations for this case are as given by equations (3.10) and (3.11). For solving the normal equations for the parameter N_{ox} (Number of Transfer Units) and the axial mixing parameter R , an iterative technique is used with the IBM/360 computer system. (See appendix F for the flow chart). But unlike the case of a one parameter model, in the two parameter model the values of the parameters N_{ox} and R failed to converge. In order to predict

the effect of introducing the axial mixing parameter R in the mathematical model, equation (3.8), an alternate method is used. For the various values of the parameter N_{ox} , the gas phase concentration is predicted by substituting in increments of the value of the axial mixing parameter R in the two parameter model. The average of the percentage deviation between this predicted value of the gas phase concentration and the experimentally determined gas phase concentration, (i.e. the AAPD), is plotted against the axial mixing term R with N_{ox} as the parameter. A program for plotting the graphs by the IBM/360 computer is shown in appendix F. The AAPD vs. R graphs with N_{ox} as the parameter are presented for all the 110 runs and displayed elsewhere⁽¹⁸⁾. Of the 110 runs, the graphs and the computed values of 18 runs are presented here and are tabulated elsewhere in this work. (See appendix G, and table D.)

IV. RESULTS AND DISCUSSION

This investigation allows one to ascertain and study the influence of axial dispersion in the liquid phase on the performance of a counter-current gas absorption column used for the carbon dioxide-water system. The conclusions arrived at are tentative, of course, since only set of data was available for analysis.

A. One-Parameter Model: (Piston flow in both the phases)

(i) In his experimental work, Brittan⁽²⁾ measured the concentration of carbon dioxide in the gas phase, at various points, along the length of the column. Using a Runge-Kutta method of step-wise integration, Brittan⁽²⁾ computed the concentration of carbon dioxide in the liquid phase. He calculated the NTU, HTU, and $K_L a$ values from the following equation:

$$NTU = \frac{y_1}{y_0} \int \frac{dy}{(y^* - y)} = \frac{K_L a \cdot \rho_y \cdot L}{F_y} = \frac{L}{HTU}$$

where

y = Solute concentration in liquid phase, (lb. mole solute/lb. mole solvent)

y^* = Equilibrium solute concentration in liquid phase, (lb. mole solute/lb. mole solvent)

0 = Lower terminal conditions

1 = Upper terminal conditions

F_y = Superficial mass liquid rate, (lb.)/(hr.)(sq. ft.)

ρ_y = Density of liquid, (lb./cu. ft.)

L = Total height of packing, (ft.)

HTU = Apparant height of an overall transfer unit (ft.)

$K_L a$ = Apparant capacity overall transfer coefficient (lb. mole)/(hr.)(cu. ft.)
(lb. mole/cu. ft.)

(ii) In this work, the concentration of carbon dioxide in the gas phase (Brittan's data) is substituted in the mathematical model, equation (3.3), and the model is curve-fitted by the method of least squares. Using this non-linear iterative procedure, the value of the parameter N_{ox} (i.e. the number of transfer units) does converge for all the 110 runs.

The values of NTU and HTU obtained by this method are very close to those obtained by Brittan in his work on the one-parameter system.

B. Two-Parameter Model:

(i) Brittan, also, investigated the effect of axial mixing in the gas phase (with plug flow in the liquid phase) on the performance of the gas absorption column. Upon analysing the results, he found that the influence of the gas phase dispersion on the performance is only moderately adverse and that in his opinion it is improbable that the effect is large enough to account for the differences between industrial scale performance and that predicted from available mass transfer correlations based upon small diameter columns.

(ii) Proceeding further in this work, the effect of axial mixing in the liquid phase and plug flow in the gas phase for the carbon dioxide water system was investigated. The two parameter mathematical model which takes into consideration axial dispersion in the liquid phase is curve-fitted to the experimental data of Brittan by the method of least squares. A

non-linear, iterative procedure is used. Unlike the case of the one-parameter mathematical model, when using the two-parameter model, the values of the parameter N_{ox} (i. e. the number of transfer units) and the parameter R (i. e. water phase axial mixing term) obtained in the iterative search fail to converge. When the value of R in the 'normal equations', equations (3.10) and (3.11), derived from the two-parameter mathematical model, equation (3.9), exceeds 167, the exponential values in the 'normal equations' "overflow" beyond the maximum magnitude which the IBM computer 360 can operate.

As an alternate approach to this non-converging iterative procedure, computer plotting is employed to plot AAPD for the two parameter mathematical model as a function of the curve-fitting parameters N_{ox} and R which serves to visually elucidate the effect of the axial mixing parameter on the performance of the column. These plots are prepared for each of the 110 runs. As speculated by Brittan, examination of these graphs for the various experimental runs depicted little significance of the axial mixing parameter R upon the performance of the tower.

C. Applicability of the Models:

From the figures shown (i. e. from G 1 to G 18), it is possible to obtain the values of average absolute percentage deviation for each value of N_{ox} corresponding to various values of R. For each value of N_{ox} , it is noted that as the value of R is increased from 1 to 100 the value of AAPD remains almost constant for the values of R greater than about 20. (i. e. when the axial dispersion in the liquid phase reduces); note that when the value of R tends to infinity, axial dispersion in the liquid phase disappears and the

liquid flow regime is characterised by the conditions of plug flow. For most of the runs, the value of AAPD increases when the value of R is decreased below 20. In the mathematical model studied here, equation (3.9), which considers the case of axial mixing in the liquid phase, the value of the AAPD decreases as the value of R increases and then remains constant, i.e. when the liquid phase axial mixing case tends towards the case of plug flow. The above-mentioned characteristics are seen in the Figures G 14, G 40, G 92, G 10, G 18, G 34, G 45, etc.

The minimum value of the AAPD obtained from the graph for each run is very close to the values of AAPD computed by the non-linear regression analysis of the mathematical model, equation (3.3), for the case of plug flow in both the gas and the liquid phases. As a result, the introduction of the liquid-phase, axial mixing parameter in the mathematical model, equation (3.8), has no effect in fitting the curve closer to the experimental data. Hence, the eddy diffusivity in the liquid phase for the carbon dioxide water system, based on the data obtained by Brittan, has little significance as far as the performance of the gas-absorption column is concerned.

V. SUMMARY AND CONCLUSION

The purpose of the present work has been to investigate whether the axial mixing in the liquid phase, for the carbon-dioxide water system, has any adverse effect on the performance of the absorption tower. The conclusions were drawn by comparing the results with that obtained by assuming plug flow in the liquid phase. In both the cases piston flow was assumed in the gas phase. Michael Brittan and Edward Woodburn⁽²⁾ had considered the case of axial mixing in the gas phase. This investigation lends further support to Michael Brittan's prediction that the discrepancy between the actual absorption column performance and that predicted from standard mass transfer correlations is due primarily to axial dispersion of the gas phase.

The experimental data for the present investigation were obtained from Michael Brittan's⁽¹⁾ work on the absorption of carbon-dioxide by water in a packed column. In this study, the gas rate was from 3.5 lb/(hr.)(sq. ft.) to 9.5 lb./(hr.)(sq. ft.) and the liquid rate from 2,500 lb./(hr.)(sq. ft.). The absorption tower consisted of a single 3 5/8 inch I.D. glass section with 1/2 inch Raschig rings as the packings; the overall packed height was 34.75 inches. The carbon dioxide concentration was measured at five different heights along the length of the column in addition to the inlet and the outlet of the column.

The mathematical models used for the plug flow and the axial mixing cases were obtained from the work of Miyauchi⁽¹³⁾. For the plug flow case, the parameter N_{ox} , (i.e. the Number of Transfer Units) was obtained by the use of the method of least squares. For the axial mixing case the axial mixing parameter R and the number of transfer units parameter N_{ox} were obtained by

graphical method. (A non-linear least square approach was attempted, but the solution did not converge.)

When analysing the data in terms of plug flow in the liquid phase, it was observed that the number of transfer units and the height equivalent to a transfer unit obtained for the various runs by the method of least squares were very close to those obtained by Brittan by a Runge-Kutta method of step-wise integration. At various heights along the length of the column, Brittan computed the concentration of carbon-dioxide in the liquid phase from which he obtained the NTU values. Whereas in this work, the concentration of carbon dioxide in the gas phase was employed to obtain the NTU values.

In the mathematical model for the case of axial mixing in the liquid phase, the value of the axial mixing parameter R was increased from 1 to 100, and that of the number of transfer units N_{ox} , from 0.27 to 1.43. Corresponding to these various permutations of R and N_{ox} the values of the carbon dioxide concentration in the gas phase were predicted along the length of the column. The percentage deviation of these predicted values of the gas phase concentration from the experimentally determined values was plotted against the liquid mixing term R with N_{ox} as the parameter for each of the 110 runs. All these plots exhibited a general trend; the value of the average absolute percentage deviation remained almost constant, irrespective of the value of the mixing parameter R , beyond the range of R equal to 20. For every individual value of N_{ox} the graph approached a minimum AAPD; and for every individual run, there was one unique value of N_{ox} and R where the value of AAPD was minimum. For the individual runs this value of the minimum AAPD remained close to the

value of the AAPD obtained from the plug flow case. This closeness between the values of AAPD meant that by introducing the axial mixing parameter R , in the mathematical model it was not possible to reduce the deviation between the predicted value and the experimental data. In other words, the axial mixing parameter R in the liquid phase had no significant effect in fitting the curve more closely to the experimental values. The above results lead to the conclusion that the effect of liquid mixing is negligible on the performance of the absorption column for the carbon-dioxide water system.

VI. APPENDICES

APPENDIX A

Derivation of the boundary conditions for the absorption column:

A. X Phase:

1. Bottom of the column:

Taking a material balance at the section shown in Figure A.1

input - output + generation = accumulation

$$\begin{aligned}
 & \left[U_x A_c \rho_x c_x \Delta t - E_x \frac{d(\rho_x c_x)}{dz} A_c \Delta t \right]_{z=0} - \frac{\Delta z}{2} \\
 & - \left[U_x A_c \rho_x c_x \Delta t - E_x \frac{d(\rho_x c_x)}{dz} A_c \Delta t \right]_{z=L} + \frac{\Delta z}{2}
 \end{aligned} \tag{A.1}$$

$$+ \left[-K_x a A_c dz (c_x - c_x^*) \Delta t \right]_{z=0} + \frac{\Delta z}{4} = 0$$

Since there is no absorption of the gas below the bed, (i.e. below $z = 0$), the 'generation' term is zero. Rearranging the equation (A.1),

$$\left[U_x c_x - E_x \frac{dc_x}{dz} \right]_{z=0} - \left[U_x c_x - E_x \frac{dc_x}{dz} \right]_{z=L} = 0 \tag{A.2}$$

expanding the terms,

$$\left[U_x c_x - E_x \frac{dc_x}{dz} \right]_{z=0} - \left[U_x c_x - E_x \frac{dc_x}{dz} \right]_{z=L} = 0 \tag{A.3}$$

at $z < 0$, $c_x = c_{x0}$; eddy diffusivity $E_x = 0$;

therefore

$$U_x c_{x0} - \left[U_x c_x - E_x \frac{dc_x}{dz} \right]_{z=0} = 0 \tag{A.4}$$

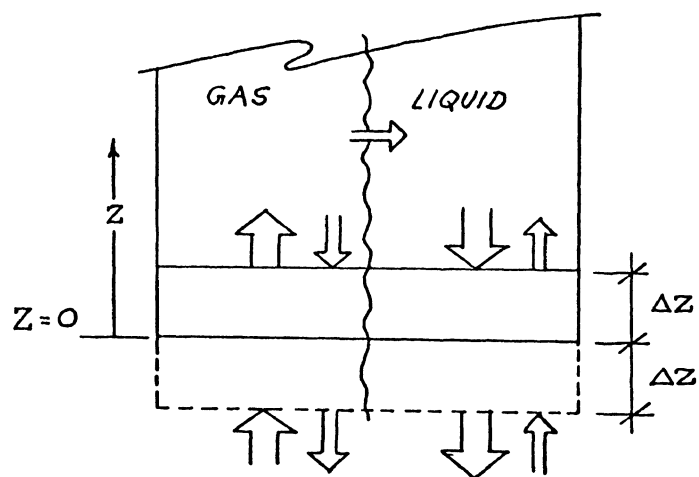


Figure A.1 Gas and Liquid Flow Regimes at the Bottom of an Absorption Tower.

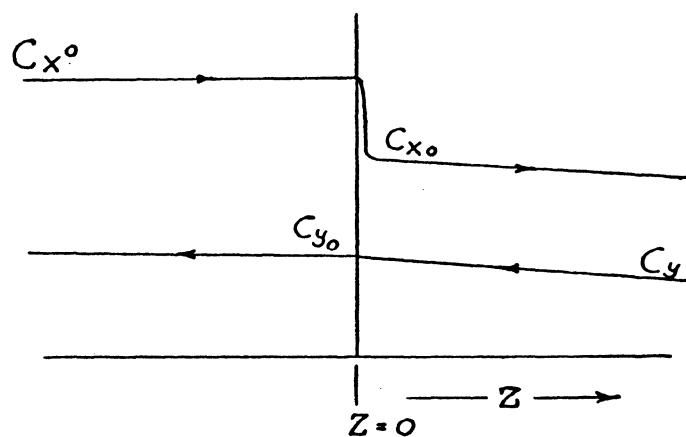


Figure A.2 Concentration Profile, of the Gas and the Liquid Phases, at the Bottom of the Absorption Tower.

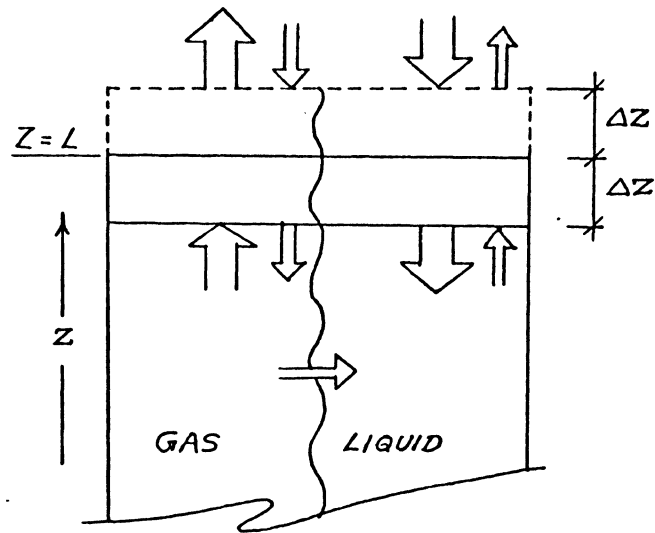


Figure A.3 Gas and liquid Flow Regimes at the Top of an Absorption Tower.

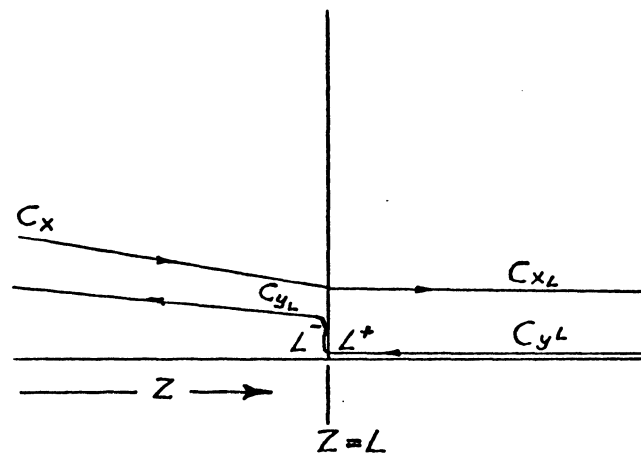


Figure A.4 Concentration Profile, of the Gas and the Liquid Phases, at the Top of the Absorption Tower.

Rearranging the equation (A. 4),

$$\frac{U_x}{E_x} (c_{x0} - c_x) = - \frac{dc_x}{dz} \quad (\text{A. 5})$$

Writing equation (A. 5) into a dimensionless form by substituting $C_x = \frac{c_x}{c_{x0}}$ and $Z = \frac{z}{L}$

$$\frac{U_x L}{E_x} (1 - C_x) = - \frac{dC_x}{dZ} \quad (\text{A. 6})$$

$$\text{But } \frac{U_x L}{E_x} = P_x B; \quad (\text{A. 7})$$

$$P_x B (1 - C_x) = - \left(\frac{dC_x}{dZ} \right) \quad (\text{2. 3})$$

Equation (2. 3) is the boundary condition for the X phase at the bottom of the column.

2. Top of the column:

Taking a material balance at the section shown in the Figure A. 3,

$$\begin{aligned} & [U_x A_c \rho_x c_x \Delta t - E_x \rho_x \frac{dc_x}{dz} A_c \Delta t]_{L - \frac{\Delta z}{2}} \\ & - [U_x A_c \rho_x c_x \Delta t - E_x \rho_x \frac{dc_x}{dz} A_c \Delta t]_{L + \frac{\Delta z}{2}} \\ & + [-K_x a A_c dz (c_x - c_x^*) \Delta t]_{L - \frac{\Delta z}{4}} = 0 \end{aligned} \quad (\text{A. 8})$$

Since there is no absorption of the gas above the bed, (i. e. above $z = L$), the generation term is zero. Rearranging the equation (A. 8),

$$[U_x c_x - E_x \frac{dc_x}{dz}]_{L - \frac{\Delta z}{2}} - [U_x c_x - E_x \frac{dc_x}{dz}]_{L + \frac{\Delta z}{2}} = 0 \quad (\text{A. 9})$$

since for $z > L$, the eddy diffusivity $E_x = 0$,

Therefore,

$$\left[U_x c_x - E_x \frac{dc_x}{dz} \right]_{L - \frac{\Delta z}{2}} - \left[U_x c_x \right]_{L + \frac{\Delta z}{2}} = 0 \quad (\text{A.10})$$

Rearranging the equation (A.10),

$$U_x \left[c_x \Big|_{L - \frac{\Delta z}{2}} - c_x \Big|_{L + \frac{\Delta z}{2}} \right] = E_x \left(\frac{dc_x}{dz} \right)_{L - \frac{\Delta z}{2}} \quad (\text{A.11})$$

Now during the process of absorption the gas (i.e. X phase) concentration decreases as the gas travels up the column, and so,

$$c_x \Big|_{L - \frac{\Delta z}{2}} \geq c_x \Big|_{L + \frac{\Delta z}{2}} \quad (\text{A.12})$$

i.e.

$$c_x \Big|_{L - \frac{\Delta z}{2}} - c_x \Big|_{L + \frac{\Delta z}{2}} \geq 0 \quad (\text{A.13})$$

From the Figure A.4 note that

$$\left(\frac{dc_x}{dz} \right)_{L - \frac{\Delta z}{2}} \leq 0 \quad (\text{A.14})$$

To satisfy both (A.13) and (A.14), both must be equal to zero.

i.e.

$$c_x \Big|_{L^-} = c_x \Big|_{L^+} \quad (\text{A.15})$$

$$\text{and so } E_x = 0 \quad (\text{A.16})$$

i.e. eddy diffusivity is zero at the top of the column.

B. Y Phase:

The process of absorption being counter-current the Y phase (i. e. water) enters at the top of the column and leaves from the bottom of the column. By reasonings similar to case of X Phase, the following results are obtained:

1. Bottom of the column: (exit end for Y phase)

$$E_{y_1} = 0 \quad (\text{A.17})$$

i. e. eddy diffusivity in the water phase at the bottom of the column is zero.

2. Top of the column: (inlet end for Y phase)

$$P_{y_1} B (C_{y_1} - C_{y_1}) = - \left[\frac{dC_y}{dz} \right] \quad (\text{A.18})$$

where

$$C_{y_1} = \frac{c_{y_1}}{c_{x_0}} \quad (\text{A.19})$$

and

$$C_{y_1} = \frac{c_{y_1}}{c_{x_0}} \quad (\text{A.20})$$

Equation (A.18) shows the presence of eddy diffusivity in the water phase at the top of the column.

APPENDIX B

Equation of Continuity for homogeneous flow systems:

For homogeneous continuous flow systems Damkohler⁽⁷⁾ has given an equation of continuity as follows:

$$\frac{\partial c_i}{\partial \theta} = -\text{div} (-E_i \text{grad } c_i) - \text{div} (U_i c_i) + \phi(c_i) \quad (\text{B.1})$$

where U_i is the linear velocity of the fluid and c_i is the concentration of i^{th} component at the point of interest. For one-dimensional steady state flow systems, in which a mean diffusivity and a mean velocity of the i^{th} component are assumable, Damkohler's equation becomes

$$E_i \frac{d^2 c_i}{dz^2} - U_i \frac{dc_i}{dz} - \phi(c_i) = 0 \quad (\text{B.2})$$

For one-dimensional countercurrent two-phase mass transfer process this equation is modified as follows, by introducing a void fraction ϵ for each phase and substituting the mass transfer term for $\phi(c_i)$;

$$\epsilon_x E_x \frac{d^2 c_x}{dz^2} - F_x \frac{dc_x}{dz} - K_x a(c_x - mc_y) = 0 \quad (\text{B.3})$$

$$\epsilon_y E_y \frac{d^2 c_y}{dz^2} + F_y \frac{dc_y}{dz} + K_x a(c_x - mc_y) = 0 \quad (\text{B.4})$$

where the direction of mass transfer is taken from phase x to phase y and a linear distribution equilibrium (with 'm' as the partition coefficient) is assumed. K_x represents the overall mass transfer coefficient relative to phase x; 'a' is the interfacial area per unit volume, and F is the superficial velocity of the designated phase. These equations are based on a simplified model which assumes the two phases flow in opposite directions,

with each phase undergoing longitudinal dispersion. Rearranging the equation into dimensionless form we have,

$$\frac{d^2 C_x}{dZ^2} - P_x B \frac{dC_x}{dZ} - N_{ox} P_x B (C_x - mC_y) = 0 \quad (2.1)$$

and

$$\frac{d^2 C_y}{dZ^2} + P_y B \frac{dC_y}{dZ} + N_{oy} P_y B (C_x - mC_y) = 0 \quad (2.2)$$

where $C_x = \frac{c_x}{c_{x0}}$ (B.5)

$$C_y = \frac{c_y}{c_{y0}} \quad (B.6)$$

$$B = \frac{L}{d} \quad (B.7)$$

$$P_x = \frac{U_x d}{E_x} \quad (B.8)$$

$$P_y = \frac{U_y d}{E_y} \quad (B.9)$$

$$Z = \frac{z}{L} \quad (B.10)$$

$$N_{ox} = \frac{K_x a L}{F_x} \quad (B.11)$$

$$N_{oy} = \frac{K_y a L}{F_y} \quad (B.12)$$

$$U_x = \frac{F_x}{\epsilon_x} \quad (B.13)$$

$$U_y = \frac{F_y}{\epsilon_y} \quad (\text{B.14})$$

The associated boundary conditions as derived in Appendix A are as follows:

$$\text{a) } Z = 0, \quad \text{i) } -\left[\frac{dC_x}{dZ}\right] = P_x B (1 - C_x) \quad (2.3)$$

$$\text{ii) } -\left[\frac{dC_y}{dZ}\right] = 0 \quad (2.4)$$

$$\text{b) } Z = 1, \quad \text{i) } -\left[\frac{dC_x}{dZ}\right] = 0 \quad (2.5)$$

$$\text{ii) } -\left[\frac{dC_y}{dZ}\right] = P_y B (C_{y1} - C_y) \quad (2.6)$$

APPENDIX C

Normal Equation for Case 1:

$$\text{Let } C_{xi}^* = \frac{e^{\lambda z_i} - \Lambda e^\lambda}{1 - \Lambda e^\lambda} \quad (\text{C.1})$$

be the mathematical model for the case of plug flow in both the gas and the liquid phases; C_{xi}^* is the predicted value of the concentration of carbon dioxide in the gas phase, and C_{xi} is that experimentally determined.

Let the deviation between the experimental and the predicted values be $\bar{\epsilon}$

$$\text{i.e. } \bar{\epsilon}_i = (C_{xi} - C_{xi}^*) \quad (\text{C.2})$$

The best fitting curve through the data is the curve which makes the sum of the squares of deviations of the experimental C_x values from the predicted C_x^* values a minimum;

$$\text{i.e. } S = \sum_{i=1}^n (\bar{\epsilon}_i)^2 \text{ is a minimum.} \quad (\text{C.3})$$

where

$$i = 1, 2, \dots, (n-1), n.$$

n = total number of data points

C_{xi} = concentration of carbon dioxide in the gas phase at the point Z_i

Z_i = height of the point i from the base of the column.

The sum of the squares of deviation is a function of N_{ox} and hence of λ .

This deviation will be a minimum when

$$\frac{dS}{d\lambda} = 0; \quad (\text{C.4})$$

$$\text{i.e. } \frac{dS}{d\lambda} = -2 \sum_{i=1}^n (C_{xi} - C_{xi}^*) \frac{\partial C_{xi}^*}{\partial \lambda} \equiv 0 \quad (\text{C.5})$$

Expanding the non-linear mathematical model, equation (C.1), in Taylor series around the point $\lambda = \lambda_0$,

$$C_{x(\lambda)}^* = \frac{e^{\lambda_0 Z} - \Lambda e^{\lambda_0}}{1 - \Lambda e^{\lambda_0}} + \left[\frac{\partial C_x^*}{\partial \lambda} \right]_{\lambda=\lambda_0} (\lambda - \lambda_0) + (\text{neglect higher order derivatives}) \quad (C.6)$$

Now taking the partial derivative of C_x^* , represented by equation (C.6), with respect to λ at $\lambda = \lambda_0$,

$$\left[\frac{\partial C_x^*}{\partial \lambda} \right]_{\lambda=\lambda_0} = \frac{(1 - \Lambda e^{\lambda_0})(Z e^{\lambda_0 Z} - \Lambda e^{\lambda_0}) - (e^{\lambda_0 Z} - \Lambda e^{\lambda_0})(-\Lambda e^{\lambda_0})}{(1 - \Lambda e^{\lambda_0})^2} \quad (C.7)$$

Rearranging the terms,

$$\left[\frac{\partial C_x^*}{\partial \lambda} \right]_{\lambda=\lambda_0} = \frac{Z e^{\lambda_0 Z} (1 - \Lambda e^{\lambda_0}) + \Lambda e^{\lambda_0} (e^{\lambda_0 Z} - 1)}{(1 - \Lambda e^{\lambda_0})^2} \quad (C.8)$$

Substituting the value of $\frac{\partial C_x^*}{\partial \lambda}$ at $\lambda = \lambda_0$, i.e. equation (C.8) in equation (C.6),

$$C_{x(\lambda)}^* = \frac{e^{\lambda_0 Z} - \Lambda e^{\lambda_0}}{1 - \Lambda e^{\lambda_0}} + \frac{Z e^{\lambda_0 Z} (1 - \Lambda e^{\lambda_0}) + \Lambda e^{\lambda_0} (e^{\lambda_0 Z} - 1)}{(1 - \Lambda e^{\lambda_0})^2} (\lambda - \lambda_0) \quad (C.9)$$

Equation (C.9) shows the mathematical model expanded in Taylor series.

Differentiating partially the mathematical model, equation (C.9), with respect to λ ,

$$\left[\frac{\partial C_x^*}{\partial \lambda} \right] = 0 + \frac{Z e^{\lambda_0 Z} (1 - \Lambda e^{\lambda_0}) + \Lambda e^{\lambda_0} (e^{\lambda_0 Z} - 1)}{(1 - \Lambda e^{\lambda_0})^2} \cdot (1-0) \quad (C.10)$$

Substituting equation (C.10) in equation (C.5) as follows:

$$\frac{ds}{d\lambda} = 0 \equiv 2 \sum_{i=1}^{\eta} \left\{ \left[C_{xi} - \frac{e^{\lambda_0 Z_i} - \Lambda e^{\lambda_0}}{(1 - \Lambda e^{\lambda_0})} - \frac{Z_i e^{\lambda_0 Z_i} (1 - \Lambda e^{\lambda_0}) + \Lambda e^{\lambda_0} (e^{\lambda_0 Z_i} - 1)}{(1 - \Lambda e^{\lambda_0})^2} (\lambda - \lambda_0) \right] \right. \\ \left. \left[\frac{Z_i e^{\lambda_0 Z_i} (1 - \Lambda e^{\lambda_0}) + \Lambda e^{\lambda_0} (e^{\lambda_0 Z_i} - 1)}{(1 - \Lambda e^{\lambda_0})^2} \right] \right\} \quad (C.11)$$

Rearranging the above-shown equation,

$$\sum_{i=1}^{\eta} C_{xi} \left[\frac{Z_i e^{\lambda_0 Z_i} (1 - \Lambda e^{\lambda_0}) + \Lambda e^{\lambda_0} (e^{\lambda_0 Z_i} - 1)}{(1 - \Lambda e^{\lambda_0})^2} \right] \\ - \sum_{i=1}^{\eta} \left[\frac{e^{\lambda_0 Z_i} - \Lambda e^{\lambda_0}}{1 - \Lambda e^{\lambda_0}} \right] \left[\frac{Z_i e^{\lambda_0 Z_i} (1 - \Lambda e^{\lambda_0}) + \Lambda e^{\lambda_0} (e^{\lambda_0 Z_i} - 1)}{(1 - \Lambda e^{\lambda_0})^2} \right] \\ = \sum_{i=1}^{\eta} \left[\frac{Z_i e^{\lambda_0 Z_i} (1 - \Lambda e^{\lambda_0}) + \Lambda e^{\lambda_0} (e^{\lambda_0 Z_i} - 1)}{(1 - \Lambda e^{\lambda_0})^2} \right]^2 (\lambda - \lambda_0) \quad (3.6)$$

Equation (3.6) represents the 'normal equation' with λ as the parameter for the case of plug flow in both the gas and the liquid phases.

APPENDIX D

Normal Equations for Case 3:

Let the mathematical model be,

$$C_x^* = H_1 e^{\lambda_1 Z} + H_2 e^{\lambda_2 Z} + H_3 e^{\lambda_3 Z} \quad (D.1)$$

Similar to Appendix C we have the sum of the squares of the deviation between the experimental and the predicted values of the concentration of carbon dioxide in the gas phase, as follows:

$$S = \sum_{i=1}^n (C_{xi} - C_{xi}^*)^2 \quad (D.2)$$

The sum of the squares of deviation is a function of N_{ox} (will be denoted as 'X') and P_B (will be denoted as 'R'). This deviation will be a minimum when the following are satisfied:

$$i) \frac{\partial S}{\partial X} = -2 \sum_{i=1}^n (C_{xi} - C_{xi}^*) \frac{\partial C_x^*}{\partial X} \equiv 0, \quad (D.3)$$

$$ii) \frac{\partial S}{\partial R} = -2 \sum_{i=1}^n (C_{xi} - C_{xi}^*) \frac{\partial C_x^*}{\partial R} \equiv 0. \quad (D.4)$$

Expanding the non-linear mathematical model represented by the equation

(D.1), in Taylor series around the points $X = X_0$ and $R = R_0$,

$$C_x^* = C_{x_0}^* + \frac{\partial C_x^*}{\partial X} \Big|_{X=X_0} (X - X_0) + \frac{\partial C_x^*}{\partial R} \Big|_{R=R_0} (R - R_0) + (\text{neglect the higher order derivatives}) \quad (D.5)$$

A. . Partial Derivatives with respect to the parameter X (i.e. N_{ox})

Differentiating partially equation (D.1) w. r. t. X,

$$\frac{\partial C_x^*}{\partial X} = \frac{\partial H_1}{\partial X} \cdot e^{\lambda_1 Z} + H_1 \cdot Z \cdot \frac{\partial \lambda_1}{\partial X} \cdot e^{\lambda_1 Z} + \frac{\partial H_2}{\partial X} \cdot e^{\lambda_2 Z}$$

$$+ H_2 \cdot Z \cdot \frac{\partial \lambda_2}{\partial X} \cdot e^{\lambda_2 Z} + \frac{\partial H_3}{\partial X} \cdot e^{\lambda_3 Z} + H_3 \cdot Z \cdot \frac{\partial \lambda_3}{\partial X} \cdot e^{\lambda_3 Z} \quad (D.6)$$

Now,

$$H_1 = \frac{DH_1}{DH} \quad (D.7a)$$

$$H_2 = \frac{DH_2}{DH} \quad (D.7b)$$

$$H_3 = \frac{DH_3}{DH} \quad (D.7c)$$

Taking the partial derivative of equation (D.7a) w. r. t. X,

$$\frac{\partial H_1}{\partial X} = \frac{DH \cdot \frac{\partial}{\partial X} \cdot DH_1 - DH_1 \cdot \frac{\partial}{\partial X} \cdot DH}{(DH)^2} \quad (D.8a)$$

Again,

$$DH_1 = h_2 h_3 \lambda_2 \left(1 + \frac{\lambda_3}{R}\right) e^{\lambda_3} - h_3 h_2 \lambda_3 \left(1 + \frac{\lambda_2}{R}\right) e^{\lambda_2} \quad (D.9a)$$

Differentiating equation (D.9a),

$$\begin{aligned} \frac{\partial DH_1}{\partial X} &= h_2 h_3 \lambda_2 \left[\left(1 + \frac{\lambda_3}{R}\right) \left(\frac{\partial \lambda_3}{\partial X}\right) e^{\lambda_3} + \frac{e^{\lambda_3}}{R} \cdot \frac{\partial \lambda_3}{\partial X} \right] \\ &+ \left(1 + \frac{\lambda_3}{R}\right) e^{\lambda_3} \left[h_2 h_3 \left(\frac{\partial \lambda_2}{\partial X}\right) + \lambda_2 \left(h_2 \frac{\partial h_3}{\partial X} + h_3 \frac{\partial h_2}{\partial X}\right) \right] \\ &- h_3 h_2 \lambda_3 \left[\left(1 + \frac{\lambda_2}{R}\right) \left(\frac{\partial \lambda_2}{\partial X}\right) e^{\lambda_2} + \frac{e^{\lambda_2}}{R} \left(\frac{\partial \lambda_2}{\partial X}\right) \right] \\ &- \left(1 + \frac{\lambda_2}{R}\right) e^{\lambda_2} \left[h_3 h_2 \left(\frac{\partial \lambda_3}{\partial X}\right) + \lambda_3 \left(h_3 \cdot \frac{\partial h_2}{\partial X} + h_2 \cdot \frac{\partial h_3}{\partial X}\right) \right] \end{aligned} \quad (D.10a)$$

Now in equation (D.1),

$$\lambda_1 = 0 \quad (D.11a)$$

$$\lambda_2 = -\left(\frac{h}{2}\right) + \sqrt{\left(\frac{h}{2}\right)^2 - k} \quad (D.11b)$$

and

$$\lambda_3 = -\left(\frac{h}{2}\right) - \sqrt{\left(\frac{h}{2}\right)^2 - k} \quad (\text{D.11c})$$

where,

$$h = N_{ox} + P_y B \equiv X + R = a \quad (\text{D.12a})$$

and

$$k = N_{ox} \cdot P_y B \cdot (1 - \Lambda) \equiv X \cdot R \cdot (1 - \Lambda) = b \quad (\text{D.12 b})$$

Differentiating partially equations (D.11b) and (D.11c) w. r. t. X,

$$\frac{\partial \lambda_2}{\partial X} = -\frac{1}{2} \cdot \frac{\partial a}{\partial X} + \frac{1}{2} \left(\frac{a^2}{4} - b\right)^{-\frac{1}{2}} \cdot \left(\frac{1}{2} \cdot a \cdot \frac{\partial a}{\partial X} - \frac{\partial b}{\partial X}\right) \quad (\text{D.13a})$$

and

$$\frac{\partial \lambda_3}{\partial X} = -\frac{1}{2} \cdot \frac{\partial a}{\partial X} - \frac{1}{2} \cdot \left(\frac{a^2}{4} - b\right)^{-\frac{1}{2}} \cdot \left(\frac{1}{2} \cdot a \cdot \frac{\partial a}{\partial X} - \frac{\partial b}{\partial X}\right) \quad (\text{D.13b})$$

where,

$$\frac{\partial a}{\partial X} = 1 \quad (\text{D.14a})$$

$$\frac{\partial b}{\partial X} = (1 - \Lambda) R \quad (\text{D.14b})$$

Again,

$$DH = DH_1 + (h_3 \lambda_3 - h_2 \lambda_2) \quad (\text{D.15})$$

$$DH_2 = +h_3 \lambda_3 \quad (\text{D.9b})$$

and

$$DH_3 = -h_2 \lambda_2 \quad (\text{D.9c})$$

Now differentiating equation (D.15) partially w. r. t. X to get the following:

$$\frac{\partial DH}{\partial X} = \frac{\partial DH_1}{\partial X} + h_3 \frac{\partial \lambda_3}{\partial X} + \lambda_3 \frac{\partial h_3}{\partial X} - h_2 \frac{\partial \lambda_2}{\partial X} - \lambda_2 \frac{\partial h_2}{\partial X} \quad (D.16)$$

Also,

$$h_1 = 1 + \lambda_1 X \quad (D.17a)$$

$$h_2 = 1 + \lambda_2 X \quad (D.17b)$$

and

$$h_3 = 1 + \lambda_3 X \quad (D.17c)$$

The partial derivatives of the above equations i. e. (D.17a), (D.17b) and (D.17c), each w. r. t. X are as shown below:

$$\frac{\partial h_1}{\partial X} = \lambda_1 + X \cdot \frac{\partial \lambda_1}{\partial X} \quad (D.18a)$$

$$\frac{\partial h_2}{\partial X} = \lambda_2 + X \cdot \frac{\partial \lambda_2}{\partial X} \quad (D.18b)$$

$$\frac{\partial h_3}{\partial X} = \lambda_3 + X \cdot \frac{\partial \lambda_3}{\partial X} \quad (D.18c)$$

Partially differentiating equations (D.7b) and (D.7c),

$$\frac{\partial H_2}{\partial X} = \frac{DH \cdot \frac{\partial DH_2}{\partial X} - DH_2 \cdot \frac{\partial DH}{\partial X}}{(DH)^2} \quad (D.8b)$$

and

$$\frac{\partial H_3}{\partial X} = \frac{DH \cdot \frac{\partial DH_3}{\partial X} - DH_3 \cdot \frac{\partial DH}{\partial X}}{(DH)^2} \quad (D.8c)$$

The partial derivatives of the equations (D.9b) and (D.9c) w. r. t. X are as follows:

$$\frac{\partial DH_2}{\partial X} = h_3 \frac{\partial \lambda_3}{\partial X} + \lambda_3 \frac{\partial h_3}{\partial X} \quad (D.10b)$$

and

$$\frac{\partial DH_3}{\partial X} = -h_2 \frac{\partial \lambda_2}{\partial X} - \lambda_2 \frac{\partial h_2}{\partial X} \quad (D.10c)$$

B. Partial Derivatives with respect to the parameter R (i. e. P_y B)

Differentiating partially equation (D.1) w. r. t. R,

$$\begin{aligned} \frac{\partial C_x^*}{\partial R} &= \frac{\partial H_1}{\partial R} \cdot e^{\lambda_1 Z} + H_1 \cdot Z \cdot \frac{\partial \lambda_1}{\partial R} e^{\lambda_1 Z} + \frac{\partial H_2}{\partial R} \cdot e^{\lambda_2 Z} + H_2 \cdot Z \cdot \frac{\partial \lambda_2}{\partial R} \cdot e^{\lambda_2 Z} \\ &+ \frac{\partial H_3}{\partial R} \cdot e^{\lambda_3 Z} + H_3 \cdot Z \cdot \frac{\partial \lambda_3}{\partial R} \cdot e^{\lambda_3 Z} \end{aligned} \quad (D.19)$$

Taking the partial derivative of equation (D.7a) w. r. t. R,

$$\frac{\partial H_1}{\partial R} = \frac{DH \cdot \frac{\partial DH_1}{\partial R} - DH_1 \frac{\partial DH}{\partial R}}{(DH)^2} \quad (D.20a)$$

Differentiating equation (D.9a),

$$\begin{aligned} \frac{\partial DH_1}{\partial R} &= h_2 h_3 \lambda_2 \left[\left(1 + \frac{\lambda_3}{R}\right) \left(\frac{\partial \lambda_3}{\partial R}\right) e^{\lambda_3} + e^{\lambda_3} \left(\frac{R \cdot \frac{\partial \lambda_3}{\partial R} - \lambda_3}{R^2}\right) \right] \\ &+ \left(1 + \frac{\lambda_3}{R}\right) e^{\lambda_3} \left[h_2 h_3 \frac{\partial \lambda_2}{\partial R} + \lambda_2 \left(h_2 \frac{\partial h_3}{\partial R} + h_3 \frac{\partial h_2}{\partial R}\right) \right] \\ &- h_3 h_2 \lambda_3 \left[\left(1 + \frac{\lambda_2}{R}\right) \left(\frac{\partial \lambda_2}{\partial R}\right) e^{\lambda_2} + e^{\lambda_2} \left(\frac{R \cdot \frac{\partial \lambda_2}{\partial R} - \lambda_2}{R^2}\right) \right] \\ &- \left(1 + \frac{\lambda_2}{R}\right) e^{\lambda_2} \left[h_3 h_2 \frac{\partial \lambda_3}{\partial R} + \lambda_3 \left(h_3 \frac{\partial h_2}{\partial R} + h_2 \frac{\partial h_3}{\partial R}\right) \right] \end{aligned} \quad (D.21a)$$

Differentiating partially equations (D.11b) and (D.11c) w. r. t. R,

$$\frac{\partial \lambda_2}{\partial R} = -\frac{1}{2} \cdot \frac{\partial a}{\partial R} + \frac{1}{2} \left(\frac{a^2}{4} - b \right)^{-\frac{1}{2}} \left(\frac{1}{2} \cdot a \cdot \frac{\partial a}{\partial R} - \frac{\partial b}{\partial R} \right) \quad (\text{D.22a})$$

and

$$\frac{\partial \lambda_3}{\partial R} = -\frac{1}{2} \cdot \frac{\partial a}{\partial R} - \frac{1}{2} \left(\frac{a^2}{4} - b \right)^{-\frac{1}{2}} \left(\frac{1}{2} \cdot a \cdot \frac{\partial a}{\partial R} - \frac{\partial b}{\partial R} \right) \quad (\text{D.22b})$$

where,

$$\frac{\partial a}{\partial R} = 1 \quad (\text{D.23a})$$

$$\frac{\partial b}{\partial R} = (1 - \Lambda)X \quad (\text{D.23b})$$

Now we differentiate equation (D.15) partially w. r. t. R to get the following,

$$\frac{\partial DH}{\partial R} = \frac{\partial DH_1}{\partial R} + h_3 \frac{\partial \lambda_3}{\partial R} + \lambda_3 \frac{\partial h_3}{\partial R} - h_2 \frac{\partial \lambda_2}{\partial R} - \lambda_2 \frac{\partial h_2}{\partial R} \quad (\text{D.24})$$

The partial derivatives equations (D.17a), (D.17b) and (D.71c), each w. r. t. R

are as shown below,

$$\frac{\partial h_1}{\partial R} = X \cdot \frac{\partial \lambda_1}{\partial R} \quad (\text{D.25a})$$

$$\frac{\partial h_2}{\partial R} = X \cdot \frac{\partial \lambda_2}{\partial R} \quad (\text{D.25b})$$

$$\frac{\partial h_3}{\partial R} = X \cdot \frac{\partial \lambda_3}{\partial R} \quad (\text{D.25c})$$

Partially differentiating equations (D.7b) and (D.7c),

$$\frac{\partial H_2}{\partial R} = \frac{DH \cdot \frac{\partial DH_2}{\partial R} - DH_2 \frac{\partial DH}{\partial R}}{(DH)^2} \quad (\text{D.20b})$$

and

$$\frac{\partial H_3}{\partial R} = \frac{DH \cdot \frac{\partial DH_3}{\partial R} - DH_3 \frac{\partial DH}{\partial R}}{(DH)^2} \quad (D.20c)$$

The partial derivatives of the equations (D.9b) and (D.9c) w.r.t. R are as follows:

$$\frac{\partial DH_2}{\partial R} = h_3 \frac{\partial \lambda_3}{\partial R} + \lambda_3 \frac{\partial h_3}{\partial R} \quad (D.21b)$$

and

$$\frac{\partial DH_3}{\partial R} = -h_2 \frac{\partial \lambda_2}{\partial R} - \lambda_2 \cdot \frac{\partial h_2}{\partial R} \quad (D.21c)$$

Now for minimum deviation from equation (D.3) and (D.4),

$$\sum_{i=1}^n (C_{xi} - C_{xi}^*) \frac{\partial C_{xi}^*}{\partial X} = 0 \quad (D.3a)$$

and

$$\sum_{i=1}^n (C_{xi} - C_{xi}^*) \frac{\partial C_{xi}^*}{\partial R} = 0 \quad (D.4a)$$

Substituting equation (D.5) in the above equations,

$$\sum_{i=1}^n \left[C_{xi} - C_{x0}^* - \left(\frac{\partial C_{xi}^*}{\partial X} \right)_{X=X_0} (X - X_0) - \left(\frac{\partial C_{xi}^*}{\partial R} \right)_{R=R_0} (R - R_0) \right] \left(\frac{\partial C_{xi}^*}{\partial X} \right)_{X=X_0} = 0 \quad (D.26)$$

and

$$\sum_{i=1}^n \left[C_{xi} - C_{x0}^* - \left(\frac{\partial C_{xi}^*}{\partial X} \right)_{X=X_0} (X - X_0) - \left(\frac{\partial C_{xi}^*}{\partial R} \right)_{R=R_0} (R - R_0) \right] \left(\frac{\partial C_{xi}^*}{\partial R} \right)_{R=R_0} = 0 \quad (D.27)$$

Rearranging the above equations (D.26) and (D.27),

$$\begin{aligned}
& \Sigma C_{xi} \left(\frac{\partial C_{xi}^*}{\partial X} \right)_{X_0} - \Sigma C_{x_0}^* \left(\frac{\partial C_{xi}^*}{\partial X} \right)_{X_0} + \Sigma \left(\frac{\partial C_{xi}^*}{\partial X} \right)_{X_0}^2 \cdot X_0 + \Sigma \left(\frac{\partial C_{xi}^*}{\partial R} \right)_{R_0} \left(\frac{\partial C_{xi}^*}{\partial X} \right)_{X_0} \cdot R_0 \\
& = \Sigma \left(\frac{\partial C_{xi}^*}{\partial X} \right)_{R_0}^2 \cdot X + \Sigma \left(\frac{\partial C_{xi}^*}{\partial R} \right)_{R_0} \left(\frac{\partial C_{xi}^*}{\partial X} \right)_{X_0} \cdot R \quad (3.10)
\end{aligned}$$

$$\begin{aligned}
& \Sigma C_{xi} \left(\frac{\partial C_{xi}^*}{\partial R} \right)_{R_0} - \Sigma C_{x_0}^* \left(\frac{\partial C_{xi}^*}{\partial R} \right)_{R_0} + \Sigma \left(\frac{\partial C_{xi}^*}{\partial R} \right)_{R_0}^2 \cdot R_0 + \Sigma \left(\frac{\partial C_{xi}^*}{\partial R} \right)_{R_0} \left(\frac{\partial C_{xi}^*}{\partial X} \right)_{X_0} \cdot X_0 \\
& = \Sigma \left(\frac{\partial C_{xi}^*}{\partial R} \right)_{R_0} \left(\frac{\partial C_{xi}^*}{\partial X} \right)_{X_0} \cdot X + \Sigma \left(\frac{\partial C_{xi}^*}{\partial R} \right)_{R_0}^2 \cdot R \quad (3.11)
\end{aligned}$$

Equations (3.10) and (3.11) are the 'normal equations', for the case of plug flow in the gas phase but axial mixing in the liquid phase, with X (i.e. N_{ox}) and R (i.e. P_y) as the parameters.

APPENDIX E

Flow Chart for Case 1:

The 'normal equation' for the case of plug flow in both the gas and the liquid phases as given by the equation (3.6) is given below:

$$C_{xi} [A] - \left[\frac{e^{\lambda_o Z_i} - \Lambda e^{\lambda_o}}{1 - \Lambda e^{\lambda_o}} \right] [A] = [A]^2 (\lambda - \lambda_o) \quad (3.6)$$

where

$$[A] = \frac{Z_i e^{\lambda_o Z_i} (1 - \Lambda e^{\lambda_o}) + \Lambda e^{\lambda_o} (e^{\lambda_o Z_i} - 1)}{(1 - \Lambda e^{\lambda_o})^2} \quad (E.1)$$

The values of the various terms in the above equation (3.6) are illustrated below for run 30.

$$C_{xi} = \frac{c_{xi}}{c_{xo}} \quad \text{mole fraction} \quad (B.5)$$

where

c_{xi} = concentration of carbon dioxide in the gas phase and the point i
along the length of the column

and

c_{xo} = concentration of carbon dioxide in the gas phase at the inlet end
of the column (i.e. 0.2 g mole/mole of $\text{CO}_2 + \text{N}_2$)

$$\Lambda = m \frac{F_x}{F_y} \quad (3.4)$$

where

m = equilibrium distribution coefficient

= H /total pressure in atmosphere

H = Henry's constant

$$= 1767 \text{ atm/mole fraction}^{(11)}$$

$$\therefore m = 1767/(623.2/760) \text{ --- for run 30}$$

$$F_x = \text{superficial gas flow rate (lb. mole/hr. sq. ft.)}$$

The molecular weight of 20% mixture of carbon dioxide in nitrogen is 31.2

$$\therefore F_x = 5.74/31.2 \text{ (lb. mole/hr. sq. ft.) --- for run 30}$$

$$F_y = \text{superficial liquid flow rate (lb. mole/hr. sq. ft.)}$$

$$\therefore F_y = 7,356/18.0 \text{ (lb. mole/hr. sq. ft.) --- for run 30}$$

$$Z_i = \frac{z_i}{L} \text{ (dimensionless)} \quad (\text{B.10})$$

where

z_i = height of the packing from the base to the point i

and

L = total height of the packing (ft.)

$$= 2.895 \text{ ft.}$$

$$\text{Variance on } c_x, \sigma_{(cx)}^2 = \frac{1}{\text{D.F.}} \sum_{i=1}^n (c_{xi} - c_{xi}^*)^2 \quad (3.13)$$

where

$$\text{D.F.} = (6 - 1) \quad (3.13a)$$

$$\text{Variance on } \lambda, \sigma_{(\lambda)}^2 = \sum_{i=1}^n \frac{1}{[A]_{xi}^2} \sigma_{(cx)}^2 \quad (3.16a)$$

$$\text{Standard deviation on } N_{ox}, \sigma_{N_{ox}} = \frac{\sigma_{(\lambda)}}{(\Lambda - 1)} \quad (3.18)$$

From equation (3.12),

$$\text{AAPD} = \frac{100}{n} \sum_{i=1}^n \left[\frac{|c_{xi} - c_{xi}^*|}{c_{xi}} \right] \quad (3.12)$$

$$K_G a = \frac{N_{ox} \cdot F_x}{L} \text{ (lb. mole/hr. cu. ft. mole. fn.)} \quad (\text{E.2})$$

```

C   SOLUTION OF NORMAL EQUATION
C   ONE PARAMETER NODEL; CASE 1
C   NON LINEAR REGRESSION ANALYSIS, NOX AS PARAMETER
1   DIMENSION CX(100), A(100), B(100), U(100), V(100),
    1W(100), CSX(100), Z(100), Z1(100), SX(100)
2   N=6
3   TR=110.
4   SOX=0.
5   SAAPD=0.
6   SVARI=0.
7   SSTDV=0.
8   SSDOX=0.
9   SAKGA=0.
10  SAZ=0.
11  READ(1,10)(Z1(I), I=1, N)
12  DO 60 K=1, 110
13  READ(1,48)RUN
14  WRITE(3,49)RUN
15  READ(1,50)PT, FY, FX
16  WRITE(3,11)PT, FY, FX
17  READ(1,10)(SX(I), I=1, N)
18  WRITE(3,13)(SX(I), I=1, N)
19  WRITE(3,3)(Z1(I), I=1, N)
20  OX=2.
21  XO=.2000
22  PT=PT/760.
23  H=1767.0
24  D=H/PT
25  FY=FY/18.
26  FX=FX/31.2
27  E=2.895

```

```

28      CL=D*FX/FY
29      SL=-OX*(1.-CL)
30      DO 22 M=1,200
31      S1=0
32      S2=0
33      S3=0
34      DO 20 I=1,N
35      Z(I)=Z1(I)/E
36      CX(I)=SX(I)/XO
37      A(I)=EXP(SL*Z(I))
38      B(I)=EXP(SL)
39      U(I)=1.-CL*B(I)
40      V(I)=(Z(I)*A(I)*U(I)+CL*B(I)*(A(I)-1.))/U(I)**2
41      W(I)=(A(I)-CL*B(I))/(1.-CL*B(I))
42      S1=S1+CX(I)*V(I)
43      S2=S2+W(I)*V(I)
44      20 S3=S3+V(I)**2
45      SL1=SL+(S1-S2)/S3
46      IF (ABS(SL1**2-SL**2)-5.0E-08)30,30,31
47      31 SL=SL1
48      22 CONTINUE
49      30 OX=-SL/(1.-CL)
50      WRITE(3,12)OX
51      S5=0
52      S4=0
53      DO 23 I=1,N
54      CSX(I)=(A(I)-CL*B(I))/(1.-CL*B(I))
55      CSX(I)=CSX(I)*XO
56      S5=S5+(ABS(SX(I)-CSX(I)))/SX(I)
57      23 S4=S4+(SX(I)-CSX(I))**2
58      WRITE(3,14)(SX(I),I=1,N)

```

```

59     WRITE(3, 88)(CSX(I), I=1, N)
60     VARI=S4/5.
61     AAPD=S5*100./6.
62     STDV=SQRT(VARI/S3)
63     SDOX=STDV/(CL-1.)
64     WRITE(3, 15)VARI, AAPD, STDV, SDOX
65 10  FORMAT(3F18.8)
66 11  FORMAT(4X, 'PT(MM HG)=' , F10.4, //4X, 'L(LB/HR. SQFT)=' F10.4, //, 4X,
      7'G(LB/HR. SQFT)=' F10.4, ///)
67 12  FORMAT(///, 4X, 'NOX='E18.8, ///)
68 13  FORMAT(2X, 'CX=' , 6F14.7)
69   3  FORMAT(2X, '7 =' , 6F14.7)
70 14  FORMAT(2X, 'CX      ', 2X, 6F18.8)
71 88  FORMAT(2X, 'CX(CAL)', 2X, 6E18.8)
72 15  FORMAT(///, 4X, 'VARIANCE**2='E18.8, //, 4X, 'AAPD          ='E18.8
      2//, 4X, 'S.DEVIATION='E18.8, //, 4X, 'S.DEV-NOX    ='E18.8//)
73 48  FORMAT(F10.4)
74 49  FORMAT('1', 2OX, 'RUN=' , F5.0, ////)
75 50  FORMAT(3F18.8)
C     CALCULATION OF HEIGHT OF THE TOWER
76     X1=0.2
77     READ(1, 200)X2
78     Y2=0.
79     CIN=X1/(1-X1)
80     COUT=X2/(1-X2)
81     CABSQB=FX*(1-X1)*(CIN-COUT)
82     Y1=CABSQB/(FY+CABSQB)
83     Y1EQ=Y1*D
84     DBOT=X1-Y1EQ
85     DTOP=X2
86     DP=(DBOT-DTOP)/ALOG(DBOT /DTOP)

```

```

87      AKGA=OX*FX/E
88      AZ=CABSOB/(AKGA*DP)
89      WRITE(3,201)CABSOB
90      WRITE(3,202)Y1
91      WRITE(3,203)Y1EQ
92      WRITE(3,204)DP
93      WRITE(3,205)AKGA
94      WRITE(3,206)AZ
95      SOX=SOX+OX
96      AOX=SOX/TR
97      SVARI=SVARI+VARI
98      AVARI=SVARI/TR
99      SAAPD=SAAPD+AAPD
100     AAAPD=SAAPD/TR
101     SSTDV=SSTDV+STDV
102     ASTDV=SSTDV/TR
103     SSDOX=SSDOX+SDOX
104     ASDOX=SSDOX/TR
105     SAKGA=SAKGA+AKGA
106     AAKGA=SAKGA/TR
107     SAZ=SAZ+AZ
108     AAZ=SAZ/TR
109     200 FORMAT(F18.8)
110     201 FORMAT(/,4X,'CO2 ABSORBED(LBMOLE/HR.SQFT)      ='F18.8)
111     202 FORMAT(/,4X,'Y1(CO2 MOLE FN IN H2O AT BOTTOM)   ='F18.8)
112     203 FORMAT(/,4X,'EQUILIBRIUM MOLE FN AT BOTTOM     ='F18.8)
113     204 FORMAT(/,4X,'LOG MEAN DRIVING FORCE(MOLE FN)    ='F18.8)
114     205 FORMAT(/,4X,' KGA LBMOLE/HR.CUFT. MOLE FN     ='F18.8)
115     206 FORMAT(/,4X,'ACTUAL HEIGHT OF COLUMN REQD     ='F18.8)
116     60 CONTINUE
117     WRITE(3,400)

```

```
118     WRITE(3,401)AOX, AVARI, AAPD, ASTDV, ASDOX, AAKGA, AAZ
119 400 FORMAT('1',10X,'AVERAGE AVLUES',////)
120 401 FORMAT(//,4X,'NOX      =',E18.8, //, 4X,'VARIANCE**2=',E18.8, //,
      24X,'AAPD      =',F18.8, //, 4X,'S.DEVIATION=',E18.8, //, 4X,'S.DEV-NO
      3X =',E18.8, 4X,'KGA      =',F18.8, //, 4X,'HEIGHT      =',F18.8)
121     STOP
122     END
/ DATA
```

TABLE I

Data Selected for the Study

[The following table shows the experimental data of Brittan⁽¹⁾ that have been used in this work:]

RUN	GAS(LB./HR.SQ.FT.)	LIQUID(LB./HR.SQ.FT.)	TOTAL PRESSURE (M.M.HG.)
20	9.5830	9195.0000	623.5000
25	9.5780	7356.0000	623.0000
36	9.5750	5517.0000	623.0000
48	9.5880	3678.0000	623.8000
14	7.6680	9195.0000	623.6001
28	7.6770	7356.0000	624.3999
40	7.6420	5517.0000	621.5000
52	7.6700	3678.0000	623.8000
92	7.6610	2298.7500	623.1001
10	5.7470	9195.0000	623.2000
30	5.7470	7356.0000	623.2000
43	5.7550	5517.0000	624.1001
55	5.7550	3678.0000	624.1001
89	5.7490	2298.0000	623.3999

TABLE I (continued)

RUN	GAS(LB./HR.SQ.FT.)	LIQUID(LB./HR.SQ.FT.)	TOTAL PRESSURE (M.M.HG.)
18	3.8300	9195.0000	623.0000
34	3.8220	7356.0000	621.8000
45	3.8270	5517.0000	622.6001
57	3.8280	3678.0000	622.7000

TABLE II

Concentration of Carbon Dioxide in Gas Phase, Experimental Against Predicted

[The following table shows the concentration of carbon dioxide (mole fraction units), in the gas phase; those experimentally determined against those predicted from the one parameter mathematical model.] (Case 1)

RUN	HEIGHT (FT.)	0.26300000	0.91699990	1.40799900	1.87500000	2.56299900	2.89500000
20	CX(EXP)	0.19539990	0.17979990	0.17159990	0.15770000	0.13029990	0.12540000
	CX(CAL)	0.19386040	0.17812800	0.16586630	0.15383360	0.13542380	0.12623940
25	CX(EXP)	0.19379990	0.18370000	0.16970000	0.16060000	0.13840000	0.12919990
	CX(CAL)	0.19475100	0.18083170	0.16951410	0.15800570	0.13962380	0.13010160
36	CX(EXP)	0.19580000	0.18739990	0.17860000	0.16850000	0.15249990	0.14279990
	CX(CAL)	0.19618240	0.18573990	0.17691920	0.16765730	0.15227710	0.14403590
48	CX(EXP)	0.19520000	0.19040000	0.18500000	0.17599990	0.16439990	0.16019990
	CX(CAL)	0.19755570	0.19057600	0.18436240	0.17754350	0.16559410	0.15888730
14	CX(EXP)	0.19620000	0.17610000	0.15700000	0.14190000	0.11809990	0.11100000
	CX(CAL)	0.19196210	0.17187600	0.15670880	0.14220970	0.12072270	0.11029910
28	CX(EXP)	0.19270000	0.17869990	0.16409990	0.15079990	0.12879990	0.11830000
	CX(CAL)	0.19338670	0.17635040	0.16298500	0.14979610	0.12948190	0.11928850
40	CX(EXP)	0.19419990	0.18430000	0.17229990	0.15869990	0.13749990	0.12989990
	CX(CAL)	0.19495890	0.18137680	0.17011510	0.15847360	0.13950440	0.12950640

TABLE II (continued)

		HEIGHT (FT.)					
		0.2630000	0.9169990	1.4079990	1.8750000	2.5629990	2.8950000
RUN							
52	CX(EXP)	0.19520000	0.18739990	0.17849990	0.16990000	0.15920000	0.15299990
	CX(CAL)	0.19687650	0.18817470	0.18065750	0.17261430	0.15894780	0.15147870
92	CX(EXP)	0.19639990	0.19029990	0.18449990	0.17809990	0.17009990	0.16879990
	CX(CAL)	0.19815020	0.19272630	0.18774020	0.18211790	0.17193400	0.16605400
10	CX(EXP)	0.19129990	0.16530000	0.14380000	0.12300000	0.09840000	0.08399999
	CX(CAL)	0.18850080	0.16103290	0.14142470	0.12354420	0.09850448	0.08695251
30	CX(EXP)	0.19010000	0.16890000	0.15049990	0.13539990	0.10559990	0.09630001
	CX(CAL)	0.19048720	0.16694520	0.14937620	0.13274910	0.10840100	0.09671396
43	CX(EXP)	0.19349990	0.17519990	0.15869990	0.14380000	0.11919990	0.10799990
	CX(CAL)	0.19269690	0.17368100	0.15856480	0.14348230	0.11993900	0.10798530
55	CX(EXP)	0.19470000	0.18209990	0.16960000	0.15670000	0.14440000	0.13830000
	CX(CAL)	0.19557470	0.18344670	0.17317830	0.16237590	0.14439510	0.13474080
89	CX(EXP)	0.19620000	0.18879990	0.18110000	0.17119990	0.16089990	0.15729990
	CX(CAL)	0.19743930	0.19001280	0.18327520	0.17576240	0.16233930	0.15467880
18	CX(EXP)	0.18489990	0.15109990	0.12089990	0.09670001	0.06110000	0.04950000
	CX(CAL)	0.18167870	0.14151410	0.11580240	0.09439147	0.06749457	0.05624033

TABLE II (continued)

		HEIGHT (FT.)					
		0.2630000	0.9169999	1.4079990	1.8750000	2.5629990	2.8950000
RUN							
34	CX(EXP)	0.1858000	0.1517000	0.1279000	0.1069999	0.0756003	0.0620000
	CX(CAL)	0.1845275	0.1492170	0.1254234	0.1047461	0.0774129	0.0654374
45	CX(EXP)	0.1898000	0.1618999	0.1391000	0.1205999	0.0924001	0.0774003
	CX(CAL)	0.1881098	0.1594077	0.1386460	0.1195033	0.0923379	0.0796564
57	CX(EXP)	0.1912000	0.1726999	0.1561999	0.1395999	0.1219999	0.1147999
	CX(CAL)	0.1928312	0.1742118	0.1594557	0.1447705	0.1219177	0.1103463

TABLE III

Computed Values of One Parameter Model

[The following table shows the values of the Number of Transfer Units, AAPD, Variance, Standard Deviation, and the Overall Mass Transfer Coefficient Computed from the one parameter model;] (Case 1)

RUN	N_{ox}	AAPD	VARIANCE (c_x) ($\times 10^5$)	STD. DEVIATION (N_{ox}) ($\times 10^2$)	KGA (lb. mole)/(Hr.)(Cu. Ft.)(Mole Fn)
20	0.64130890	2.01874500	1.59893300	0.79402290	0.06804007
25	0.65309910	0.89318810	0.36413440	0.46694860	0.06925488
36	0.51620910	0.58807410	0.16027050	0.32095560	0.05472189
48	0.38662360	0.67776660	0.23036490	0.43980990	0.04104050
14	0.82541130	1.30241200	0.86703530	0.62930570	0.07007271
28	0.75470880	0.73024170	0.19366990	0.32332240	0.06414562
40	0.69280970	0.85805730	0.36236350	0.53385680	0.05861621
52	0.44776080	0.87189130	0.35624530	0.49784540	0.03802220
92	0.32735210	1.48060100	0.93000170	0.98988150	0.02776490
10	1.14163500	1.62664600	0.81416460	-0.68656980	0.07263821
30	1.05189800	1.19129000	0.40554690	-0.51932690	0.06692851
43	0.98137000	0.37025480	0.07347822	0.26370350	0.06252801
55	0.64686940	1.58296200	1.20536800	1.02715400	0.04121530
89	0.45609790	1.28357000	0.75002050	0.94917750	0.02902990

TABLE III (continued)

RUN	N _{ox}	AAPD	VARIANCE (c _x) (x 10 ⁵)	STD. DEVIATION (N _{ox}) (x 10 ²)	KGA (lb.mole)/(Hr.)(Cu. Ft.)(Mole Fn)
18	1.66582400	6.46205900	4.39802100	-1.87906900	0.07063580
34	1.54640700	2.38441200	0.68198960	-0.76027170	0.06543511
45	1.37331100	1.10799700	0.31142800	-0.54791180	0.05818670
57	0.92883240	1.91058500	1.24244300	1.02477400	0.03936460

APPENDIX F

Flow Chart for Case 3:

The 'normal equations' for the case of plug flow in the gas phase and axial mixing in the liquid phase is as represented by the equations (3.10) and (3.11). These normal equations were programmed in the IBM computer 360, for solving the parameters N_{ox} and R by a method of iteration; but the values of N_{ox} and R failed to converge. The values of the terms like m , F_x , F_y , Z_i , C_{xi} , etc. used in the computer program were same as those shown in Appendix E: i.e.

m = Henry's constant/Total pressure in atmospheres

F_x = superficial gas flow rate (lb. mole/hr. sq. ft.)

= 5.74/31.2 (lb. mole/hr. sq. ft.) --- for run 30

F_y = Superficial liquid flow rate (lb. mole/hr. sq. ft.)

= 7,356/18.0 (lb. mole/hr. sq. ft.) --- for run 30

$$Z_i = \frac{z_i}{L} \quad (\text{dimensionless}) \quad (\text{B.10})$$

where

$$L = 2.895 \text{ (ft.)}$$

$$C_{xi} = \frac{c_{xi}}{c_{xo}} \quad (\text{dimensionless mole fraction}) \quad (\text{B.5})$$

where

$$c_{xo} = 0.2 \text{ mole CO}_2/\text{mole of (CO}_2 + \text{N}_2)$$

$$\Lambda = m \frac{F_x}{F_y} \quad (\text{3.4})$$

A computer program for the above method of iteration used, is as shown below:

```

C   SOLUTION OF NORMAL EQUATIONS
C   TWO PARAMETER MODEL; CASE 3
C   NON LINEAR REG. ANALYSIS, NOX AND PYB AS PARAMETERS
1   DIMENSION SX(100), Z(100),Z(100), Z1(100), CX(100), DXC(100), DRC(100), CHX(100
    1)
2   N=6
3   DO 60 K=1, 110
4   READ(1, 48)RUN
5   WRITE(3, 49)RUN
6   READ(1, 50)PT, FY, FX
7   WRITE(3, 11)PT, FY, FX
8   READ(1, 10)(SX(I), I=1, N)
9   READ(1, 10)(Z1(I), I=1, N)
10  WRITE(3, 3)(Z1(I), I=1, N)
11  WRITE(3, 13)(SX(I), I=1, N)
12  XIN=.200
13  PT=PT/760.
14  H=1767.0
15  D=H/PT
16  FY=FY/18.
17  FX=FX/31.2
18  E=2.895
19  CL=D*FX/FY
20  X=.94
21  R=1.
22  DO 22 M=1, 200
23  A=X+R
24  B=X*R*(1-CL)
25  SL1=0.
26  SL2=-A/2. +SQRT(A**2/4. -B)
27  SL3=-A/2. -SQRT(A**2/4. -B)

```

```

28   DXA=1.
29   DXB=(1-CL)*R
30   DXSL2=-DXA/2. +SQRT(1./(A**2/4. -B))*(A*DXA/2. -DXB)/2.
31   DXSL3=-DXA/2. -SQRT(1./(A**2/4. -B))*(A*DXA/2. -DXB)/2.
32   G2=1+SL2*X
33   G3=1+SL3*X
34   DXG2=SL2+X*DXSL2
35   DXG3=SL3+X*DXSL3
36   DH1=EXP(SL3/2.)*(G2*G3*SL2*(1+SL3/R)*EXP(SL3/2) -G3*G2*SL3*(1+SL2/R
2)*EXP(SL2-SL3/2))
37   DH2=G3*SL3
38   DH3=-G2*SL2
39   DH=DH1+(G3*SL3 -G2*SL2)
40   DXDH1=EXP(SL3/2)*(EXP(SL3/2)*G2*G3*SL2*((1+SL3/R)*DXSL3+DXSL3/R)
2+EXP(SL3/2)*(1+SL3/R)*(G2*G3*DXSL2+SL2*(G2*DXG3+G3*DXG2))
3-EXP(SL2-SL3/2)*(G3*G2*SL3*((1+SL2/R)*DXSL2+DXSL2/R))
4-EXP(SL2-SL3/2)*(1+SL2/R)*(G3*G2*DXSL3+SL3*(G3*DXG2+G2*DXG3)))
41   DXDH2=G3*DXSL3+SL3*DXG3
42   DXDH3=-G2*DXSL2-SL2*DXG2
43   DXDH=DXDH1+G3*DXSL3+SL3*DXG3 -G2*DXSL2-SL2*DXG2
44   H1=DH1/DH
45   H2=DH2/DH
46   H3=DH3/DH
47   DXH1=(DH*DXDG1 -DH1*DXDH)/DH**2
48   DXH2=(DH*DXDH2 -DH2*DXDH)/DH**2
49   DXH3=(DH*DXDH3 -DH3*DXDH)/DH**2
50   DRA=1.
51   DPB=(1-CL)*X
52   DRSL2=-DRA/2. +SQRT(1./(A**2/4. -B))*(A*DRA/2. -DRB)/2.
53   DRSL3=-DRA/2. -SQRT(1./(A**2/4. -B))*(A*DRA/2. -DRB)/2.
54   DRG2=X*DRSL2

```



```

55     DRG3=X*DRSL3
56     DRDH1=EXP(SL3/2)*(EXP(SL3/2)*G2*G3*SL2*((1+SL3/R)*DRSL3+(RDRSL3-
3)-EXP(SL2-SL3/2)*G3*G2*SL3*((1+SL2/R)*DRSL2+(R*DRSL2-SL2)/R**2)
4-EXP(SL2-SL3/2)*(1+SL2/R)*(G3*G2*DRSL3+SL3*(G3*DRG2+G2*DRG3)))
57     DRDH2=G3*DRSL3+SL3*DRG3
58     DRDH3=-G2*DRSL2-SL2*DRG2
59     DRDH=DRDH1+G3*DRSL3+SL3*DRG3-G2*DRSL2-SL2*DRG2
60     DRH1=(DH*DRDH1-DH1*DRDH)/DH**2
61     DRH2=(DH*DRDH2-DH2*DRDH)/DH**2
62     DRH3=(DH*DRDH3-DH3*DRDH)/DH**2
63     SUMX1=0.
64     SUMX2=0.
65     SUMX3=0.
66     SUMX4=0.
67     SUMX5=0.
68     SUMX6=0.
69     SUMR1=0.
70     SUMR2=0.
71     SUMR3=0.
72     SUMR4=0.
73     SUMR5=0.
74     SUMR6=0.
75     DO 20 I=1, N
76     Z(I)=Z1(I)/E
77     CX(I)=SX(I)/XIN
78     DXC(I)=EXP(SL3/2)*(DXH1*EXP(-SL3/2)+DXH2*EXP(SL2*Z(I)-SL3/2)+H2*
2Z(I)*DXSL2*EXP(SL2*Z(I)-SL3/2)+DXH3*EXP(SL3*Z(I)-SL3/2)+H3*Z(I)*
3DXSL3*EXP(SL3*7(I)-SL3/2))
79     DRC(I)=EXP(SL3/2)*(DRH1*EXP(-SL3/2)+DRH2*EXP(SL2*Z(I)-SL3/2)+H2*

```

```

2Z(I)*DRSL2*EXP(SL2*Z(I)-SL3/2)+DRH3*EXP(SL3*Z(I)-SL3/2)+H3*Z(I)*
3DRSL3*EXP(SL3*Z(I)-SL3/2))
80   CHX(I)=EXP(SL3/2)*(H1*EXP(-SL3/2)+H2*EXP(SL2*Z(I)-SL3/2)+H3*EXP
2(SL3*Z(I)-SL3/2))
81   SUMX1=SUMX1+CX(I)*DXC(I)
82   SUMX2=SUMX2+CHX(I)*DXC(I)
83   SUMX3=SUMX3+DXC(I)**2*X
84   SUMX4=SUMX4+DXC(I)*DRC(I)*R
85   SUMX5=SUMX5+DXC(I)**2
86   SUMX6=SUMX6+DXC(I)*DRC(I)
87   SUMR1=SUMR1+CX(I)*DRC(I)
88   SUMR2=SUMR2+CHX(I)*DRC(I)
89   SUMR3=SUMR3+DRC(I)**2*R
90   SUMR4=SUMR4+DRC(I)*DXC(I)*X
91   SUMR5=SUMR5+DRC(I)**2
92   20 SUMR6=SUMR6+DRC(I)*DXC(I)
93   S1=SUMX1-SUMX2+SUMX3+SUMX4
94   C1=SUMX5
95   C2=SUMX6
96   S2=SUMR1-SUMR2+SUMR3+SUMR4
97   C3=SUMR6
98   C4=SUMR5
C
C   NEWTONS METHOD OF ITERATION FOR 2 VARIABLES
C
99   F(X, R)=C1*X+C2*R-S1
100  G(X, R)=C3*X+C4*R-S2
101  DFX=C1
102  DFR=C2
103  DGX=C3
104  DGR=C4

```

```

105      A1=-F(X,R)*DGR+G(X,R)*DFR
106      A2=-G(X,R)*DFX+F(X,R)*DGX
107      B1=DFX*DGR-DFR*DGX
108      DELTAX=A1/B1
109      DELTAR=A2/B1
110      WRITE(3,12)X,R
111      X=X+DELTAX/5.
112      R=R+DELTAR/10.
113      S4=0.
114      S5=0.
115      DO 23 I=1,N
116      CHX(I)=EXP(SL/2)*(H1*EXP(-SL3/2)+H2*EXP(SL2*Z(I)-SL3/2)+H3*EXP
2(SL3*Z(I)-SL3/2))
117      CHX(I)=CHX(I)*XIN
118      S5=S5+(ABS(SX(I)-CHX(I)))/SX(I)
119 23  S4=S4+(SX(I)-CHX(I))**2
120      WRITE(3,14)(SX(I),I=1,N)
121      WRITE(3,88)(CHX(I),I=1,N)
122      DF=6.-2.
123      SIGMSX=S4/DF
124      D=C1*C4-C2*C3
125      C11=C4/D
126      C22=C1/D
127      STDVX=SQRT(ABS(C11*SIGMSX))
128      STDVR=SQRT(ABS(C22*SIGMSX))
129      AAPD=S5*100./6.
130 22  WRITE(3,15)SIGMSX,AAPD,STDVR,STDVX
131 10  Format(3F18.8)
132 11  FORMAT(4X,'PT(MM HG)=' ,F10.4, //4X,'L(LB/HR.SQFT)=' F10.4, //,4X,
      7'G(LB/HR.SQFT)=' F10.4, ///)
133 12  FORMAT(///,4X,'X='E18.8, //,4X,'R='E18.8. ///)

```

```
134 13 FORMAT(2X, 'CX=', 6F14.7)
135 3  FORMAT(2X, 'Z =', 6F14.7)
136 14 FORMAT(2X, 'CX      ', 2X, 6E18.8)
137 88 FORMAT(2X, 'CX(CAL)', 2X, 6E18.8)
138 15 FORMAT(///, 4X, 'VARIANCE**2='E18.8, //, 4X, 'AAPD      ='E18.8
      2//, 4X, 'S.DEV R      ='E18.8, //, 4X, 'S.DEV-NOX  ='E18.8//)
139 48 FORMAT(F10.4)
140 49 FORMAT('1', 20X, 'RUN=', F5.0, //)
141 50 FORMAT(3F18.8)
142 60 CONTINUE
143      STOP
144      END
```

/DATA

TABLE IV

Computed Values of Two Parameter Model

[The following table shows the value of minimum AAPD against R, with N_{ox} as the parameter, for the case 3, (i.e. plug flow in the gas phase and axial mixing in the liquid phase). These values have been obtained from the graphs plotted for the various runs.] (Figures G-1 to G-18)

RUN	N_{ox}	AAPD (minimum)	R
20	1.35	1.54	35.0
25	1.23	0.71	10.0
36	1.21	0.20	6.0
48	1.15	0.65	2.0
14	1.19	1.29	25.0
28	1.17	0.40	30.0
40	1.15	0.80	18.0
52	1.13	0.45	1.0
92	1.07	0.65	1.0
10	0.81	1.34	30.0
30	0.91	1.19	31.0
43	0.99	0.42	39.0
55	1.03	0.90	2.0
89	1.07	0.68	1.0
18	0.37	5.90	16.0
34	0.41	0.55	11.0
45	0.67	0.75	30.0
57	0.89	1.05	3.0

APPENDIX G

Computer program for the graphs:

Graphs of average absolute percentage deviation against, i.e. AAPD, against the axial mixing parameter in the liquid phase, i.e. R, for the case of plug flow in the gas phase and axial mixing in the liquid phase, for the carbon-dioxide water system, have been plotted by using the UMR IBM 360 Model, 50 digital computer system and the Calcomp Digital Incremental Plotter. The mathematical model represented by the equation (3.9) was made use of for computing the values of AAPD. For each of the 110 runs, R was increased, in steps of 1, from 1 to 100. N_{ox} , which was used as the parameter for the above graphs, was varied in the steps of 0.02, from 0.30 to 1.45. Besides the graphs, the values of AAPD, R and N_{ox} were also printed in the computer output. A program for the plotter made use of in this study, which includes the main graphs of AAPD vs. R, and the printing of their values on their respective axis together with the gas and the liquid flow rates is as given below:

C AXIAL MIXING IN ABSORPTION COLUMN
C MIXING IN THE LIQUID PHASE - PLUG FLOW IN GAS PHASE
C NON LINEAR REG ANALYSIS NOX AND PYB AS PARAMETERS
C

0001 DIMENSION SX(10), Z(10), Z1(10), CX(10), CHX(10), AAPD(110)
0002 CALL PENPOS('IYER.S.P.', 9, 1)
0003 N=6
0004 READ(1, 10)(Z1(I), I=1, N)
0005 DO 700 NJ=1, 2
0006 CALL NEWPLT(1.0, 2.0, 11.0)
0007 CALL ORIGIN(1.0, 0.0)
0008 READ(1, 48)RUN
0009 READ(1, 50)PT, FY, FX
0010 READ(1, 10)(SX(I), I=1, N)
0011 XIN=.200
0012 PT=PT/760.
0013 H=1767.0
0014 D=H/PT
0015 FY1=FY/18.
0016 FX1=FX/31.2
0017 E=2.895
0018 CL=D*FX1/FY1
0019 X=1.09
0020 DO 600 KN=1, 18
0021 R=1.
0022 DO 601 KK=1, 40
0023 A=X+R
0024 B=X*R*(1-CL)
0025 SL1=0.
0026 SL2=-A/2. +SQRT(A**2/4. -B)
0027 SL3=-A/2. -SQRT(A**2/4. -B)

```

0028      G2=1+SL2*X
0029      G3=1+SL3*X
0030      DH1=EXP(SL3/2.)*(G2*G3*SL2*(1+SL3/R)*EXP(SL3/2)-G3*G2*SL3*(1+SL2/R
2)*EXP(SL2-SL3/2))
0031      DH2=G3*SL3
0032      DH3=-G2*SL2
0033      DH=DH1+(G3*SL3-G2*SL2)
0034      H1=DH1/DH
0035      H2=DH2/DH
0036      H3=DH3/DH
0037      SUM=0.
0038      DO 20 I=1, N
0039      Z(I)=Z1(I)/E
0040      CX(I)=SX(I)/XIN
0041      CHX(I)=EXP(SL3/2)*(H1*EXP(-SL3/2)+H2*EXP(SL2*Z(I)-SL3/2)+H3*EXP
2(SL3*Z(I)-SL3/2))
0042      CHX(I)=CHX(I)*XIN
0043      SUM=SUM+ABS((SX(I)-CHX(I))/SX(I))
0044      20 Z(I)=Z(I)*E
0045      AAPD(KK)=SUM*100./6.
0046      601 R=R+1.
0047      WRITE(3, 502)RUN, X, R, AAPD(KK)
0048      502 FORMAT(4F18.8)
0049      CALL TSCALE(1.0, 40.0, 7.7)
0050      CALL YSCALE(0.0, 45.0, 5.0)
0051      CALL TPLT(AAPD, 39, 1, -1)
0052      600 X=X-0.02

0053      CALL TAXIS(1.0)
0054      CALL YAXIS(0.50)
0055      CALL SYM(-0.4, 2.0, 0.21, 'AAPD', 90.0, 4)

```



```
0056 CALL SYM(3.0, -0.5, 0.21, 'R', 0.0, 1)
0057 CALL SYM(4.5, 4.7, 0.14, 'RUN', 0.0, 3)
0058 CALL SYM(4.5, 4.3, 0.14, 'L(LB/HR.SQFT)=' , 0.0, 14)
0059 CALL NUM(5.5, 4.7, 0.14, RUN, 0.0, -1)
0060 CALL NUM(6.6, 4.3, 0.14, FY, 0.0, 2)
0061 CALL SYM(4.5, 4.0, 0.14, 'G(LB/HR.SQFT)=' , 0.0, 14)
0062 CALL NUM(6.6, 4.0, 0.14, FX, 0.0, 3)
0063 R=1.
0064 DR=5.
0065 DO 801 MN=1, 8
0066 CALL NUM(TSTOIN(R), -0.14, 0.07, R, 0.0, 1)
0067 IF(ABS(R)-4. )31, 31, 32
0068 31 R=R+4.
0069 GO TO 801
0070 32 R=R+DR
0071 801 CONTINUE
0072 AAP=0
0073 DAAP=1.0
0074 DO 802 NM=1, 21
0075 CALL NUM(-0.21, YSTOIN(AAP), 0.07, AAP, 0.0, 1)
0076 802 AAP=AAP+DAAP
0077 10 FORMAT(3F18.8)
0078 48 FORMAT(F10.4)
0079 50 FORMAT(3F18.8)
0080 CALL ENDPLT
0081 700 CONTINUE
0082 CALL LSTPLT
0083 CALL EXIT
0084 END
```

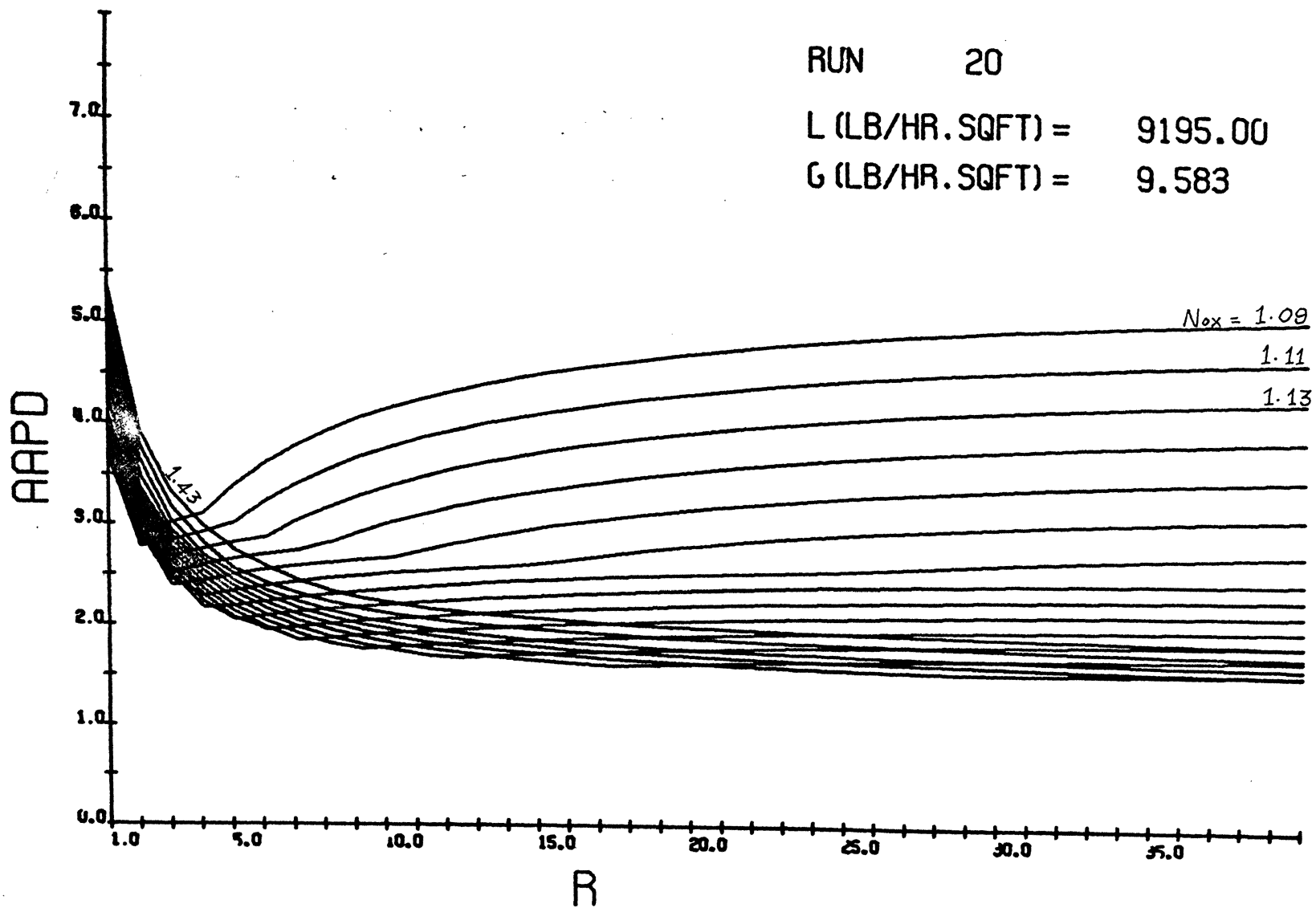


Fig. G-1. Effect of R on AAPD, N_{OX} as the parameter: Run 20. (L = 9195.00, G = 9.583, N_{OX} = 1.09 to 1.43)

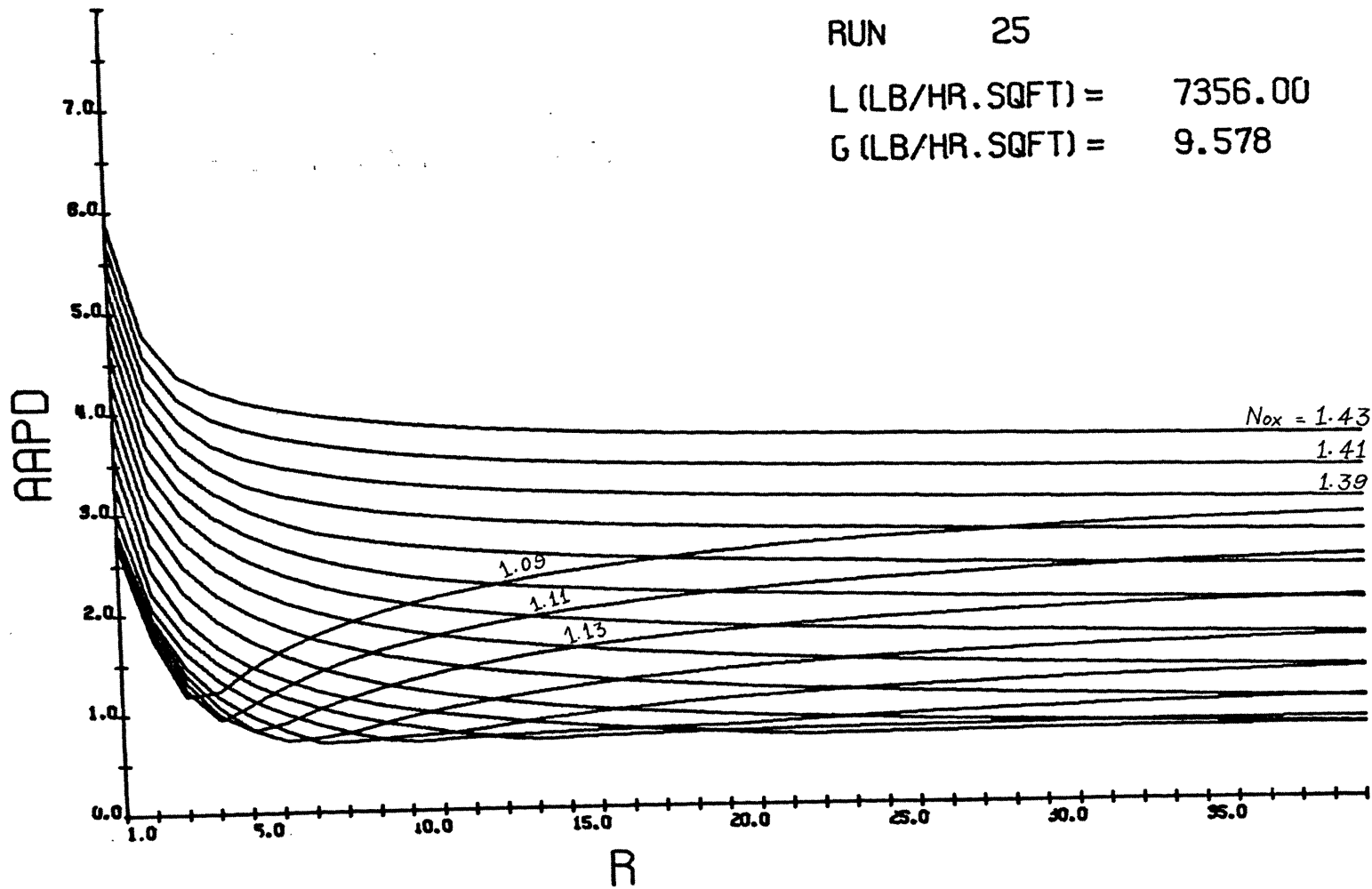


Fig. G-2. Effect of R on AAPD, N_{ox} as the parameter: Run 25. ($L = 7356.00$, $G = 9.578$, $N_{ox} = 1.09$ to 1.43)

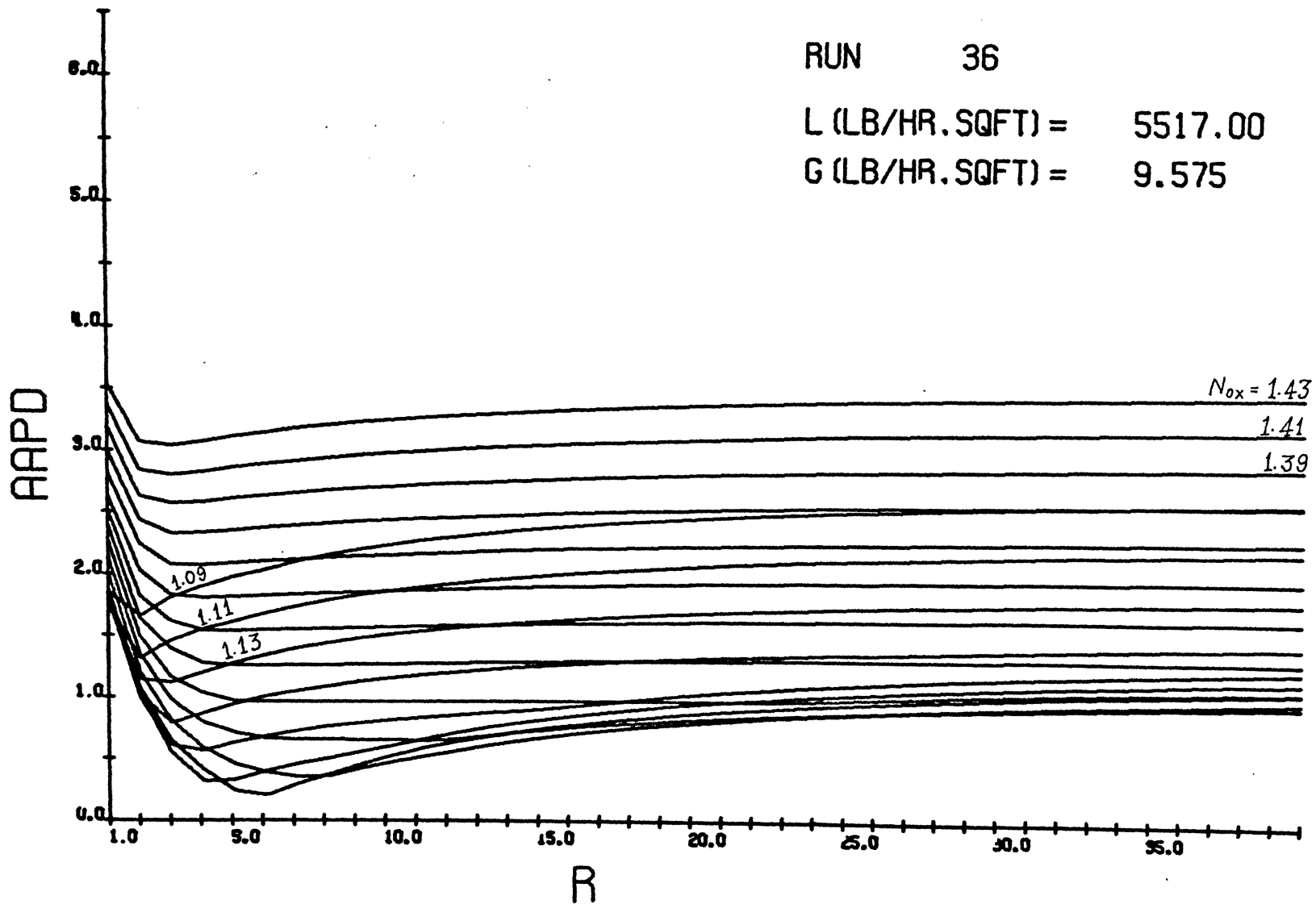


Fig. G-3. Effect of R on AAPD, N_{OX} as the parameter: Run 36. (L = 5517.00, G = 9.575, N_{OX} = 1.09 to 1.43)

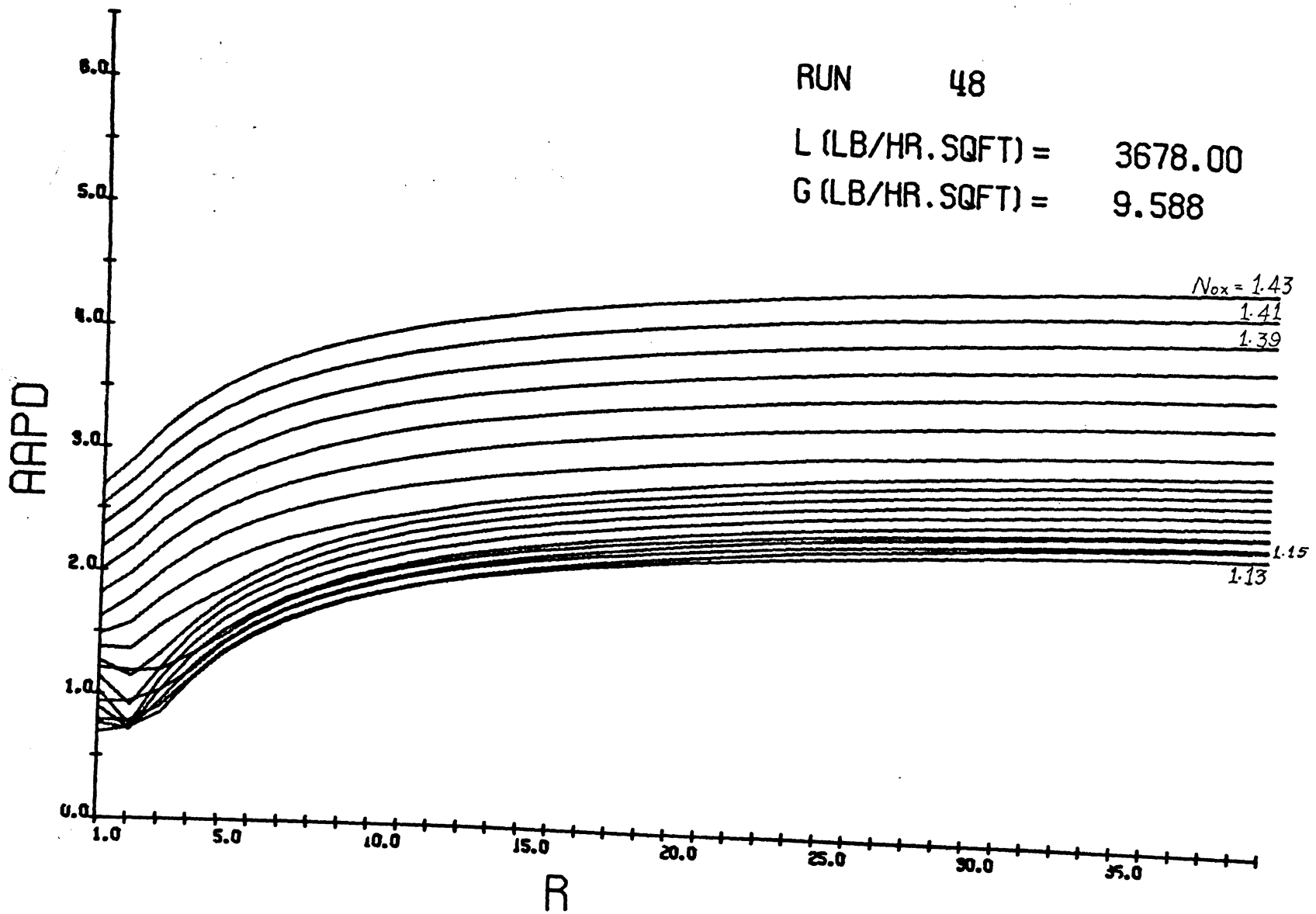


Fig. G-4. Effect of R on AAPD, N_{ox} as the parameter: Run 48. (L = 3678.00, G = 9.588, N_{ox} = 1.09 to 1.43)

RUN 14
 L (LB/HR.SQFT) = 9195.00
 G (LB/HR.SQFT) = 7.668

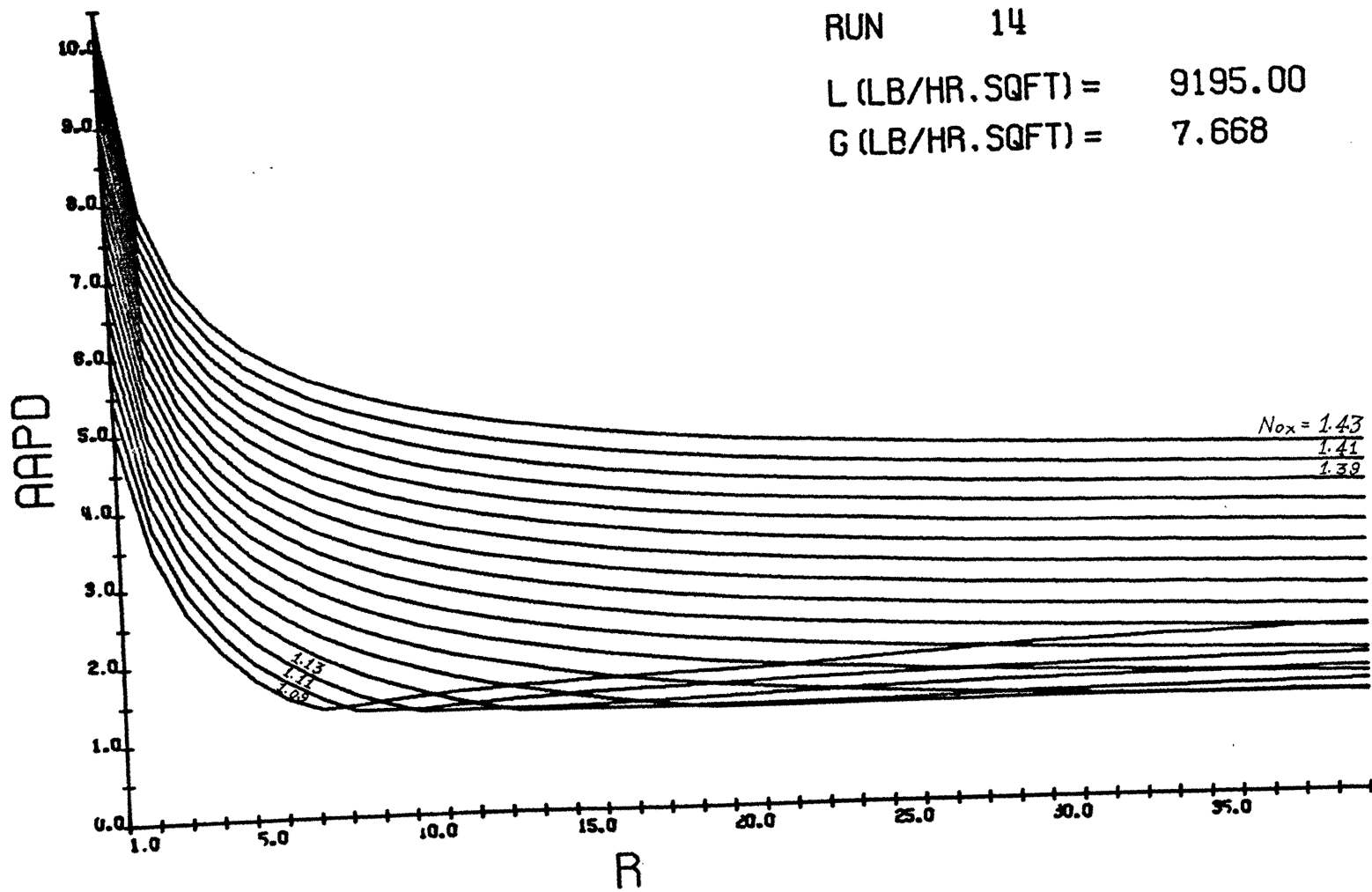


Fig. G-5. Effect of R on AAPD, N_{ox} as the parameter: Run 14. (L = 9195.00, G = 7.668, N_{ox} = 1.09 to 1.43)

RUN 28

L (LB/HR.SQFT) = 7356.00

G (LB/HR.SQFT) = 7.677

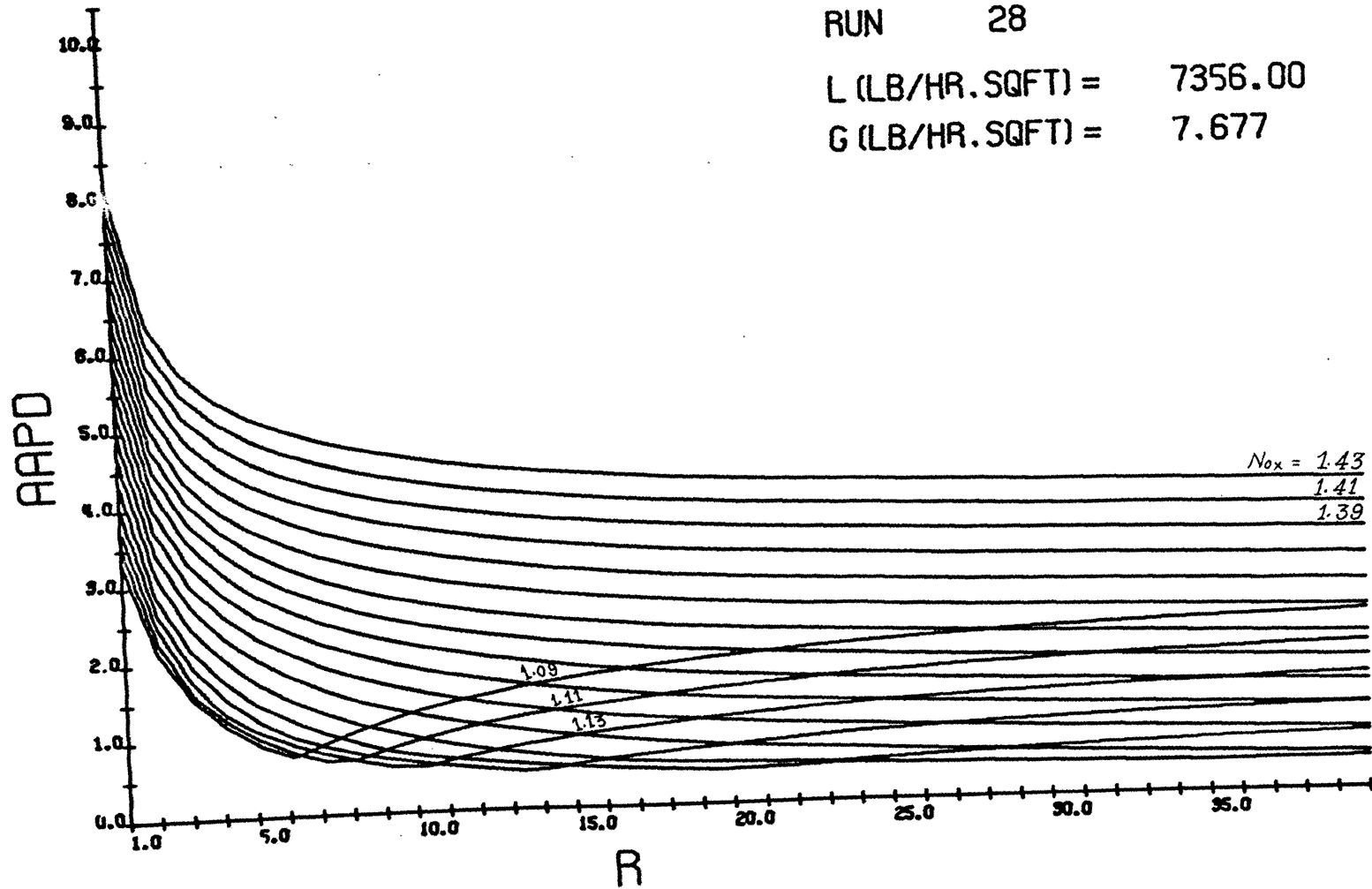


Fig. G-6. Effect of R on AAPD, N_{ox} as the parameter: Run 28. (L = 7356.00, G = 7.677, N_{ox} = 1.09 to 1.43)

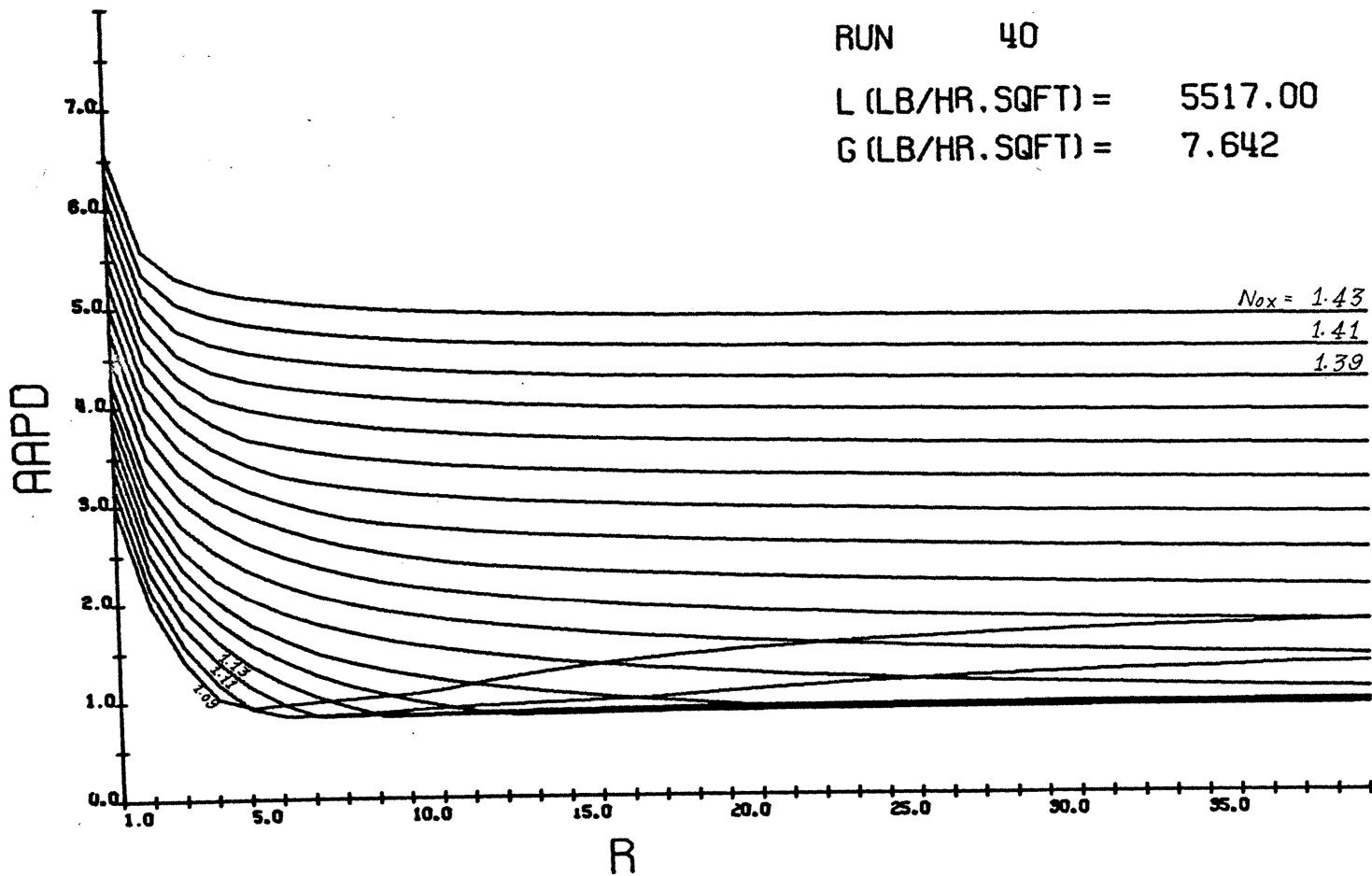


Fig. G-7. Effect of R on AAPD, N_{OX} as the parameter: Run 40. ($L = 5517.00$, $G = 7.642$, $N_{OX} = 1.09$ to 1.43)

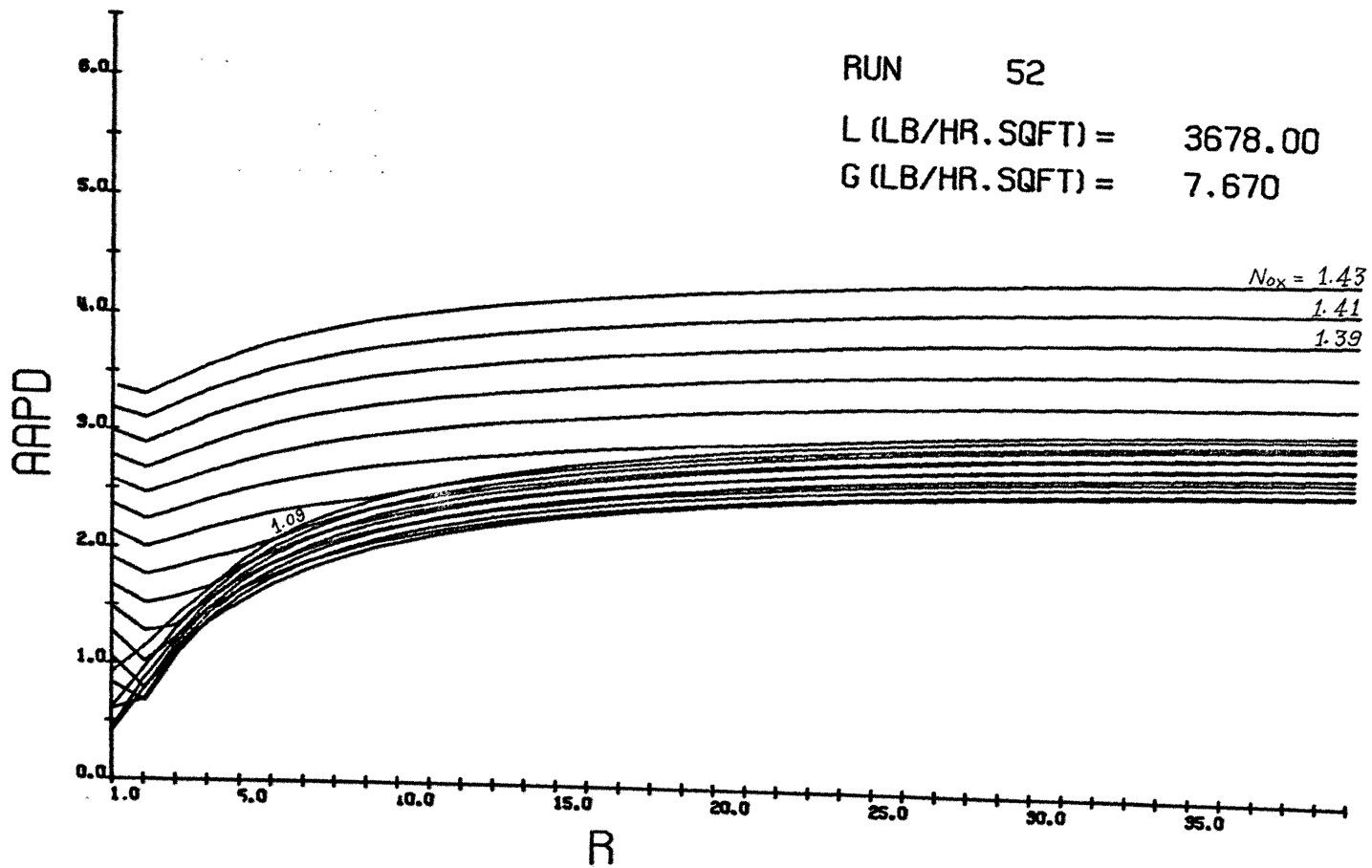


Fig. G-8. Effect of R on AAPD, N_{ox} as the parameter: Run 52. ($L = 3678.00$, $G = 7.670$, $N_{ox} = 1.09$ to 1.43)

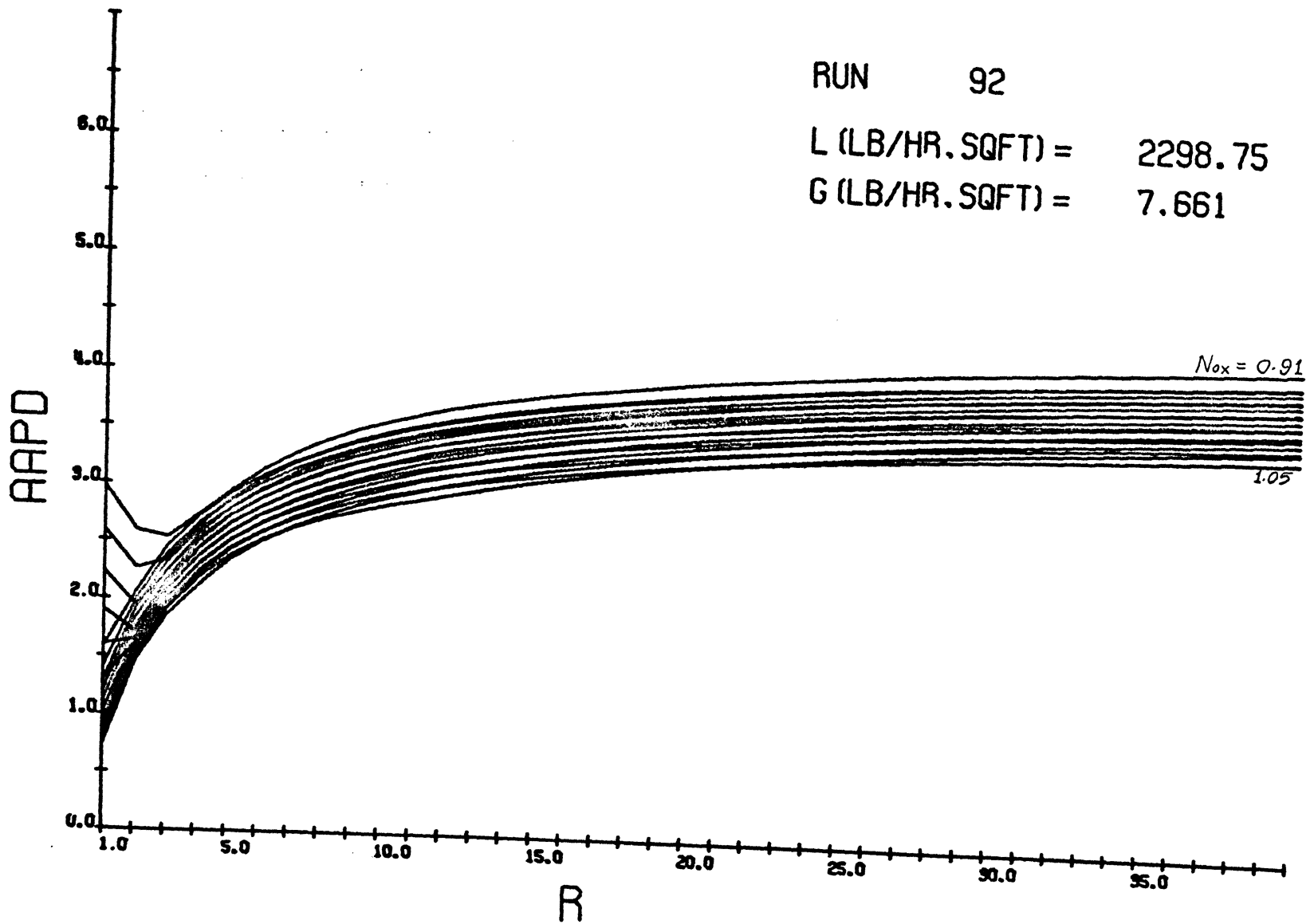


Fig. G-9. Effect of R on AAPD, N_{ox} as the parameter: Run 92. ($L = 2298.75$, $G = 7.661$, $N_{ox} = 0.91$ to 1.25)

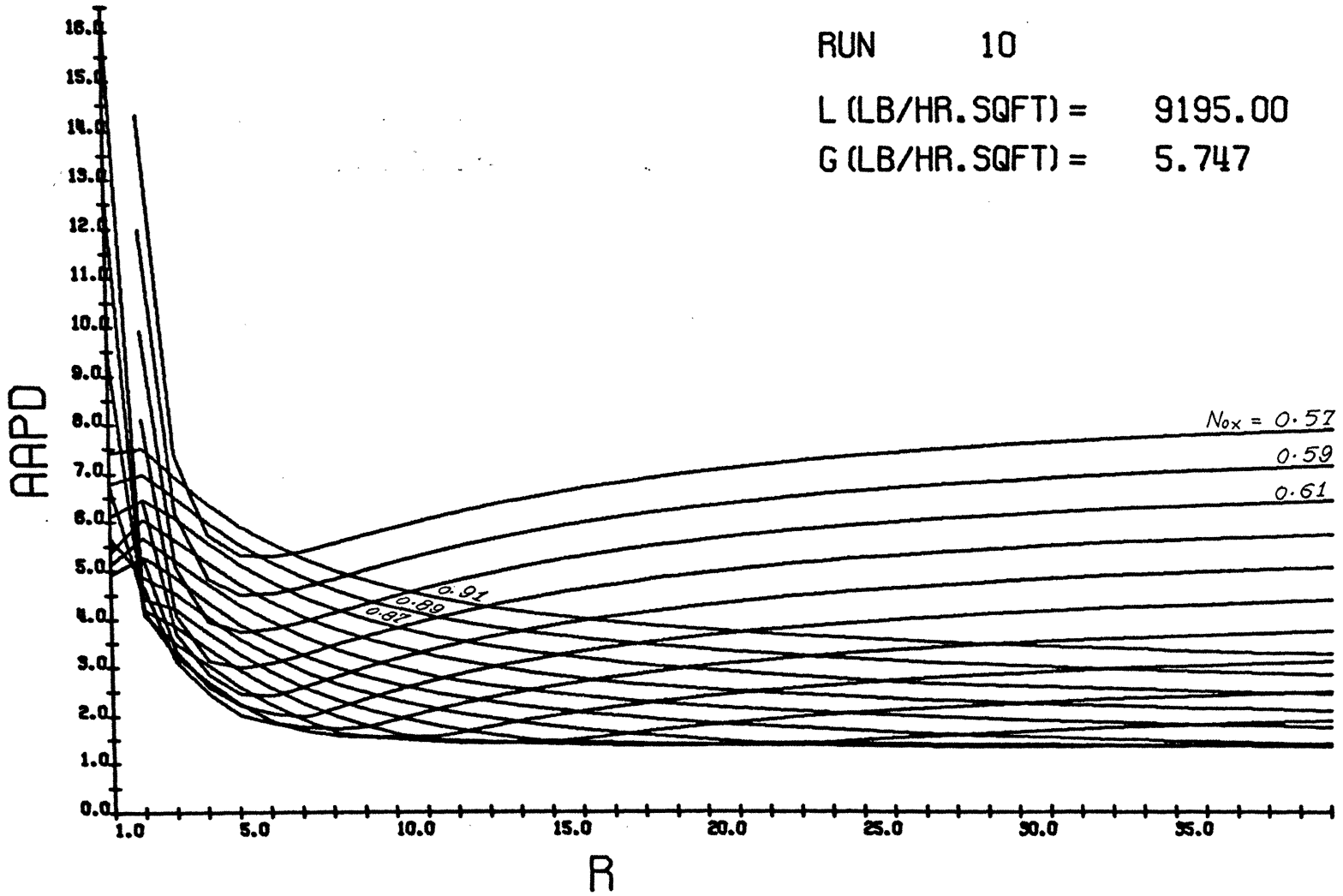


Fig. G-10. Effect of R on AAPD, N_{ox} as the parameter: Run 10. (L = 9195.00, G = 5.747, N_{ox} = 0.57 to 0.91)

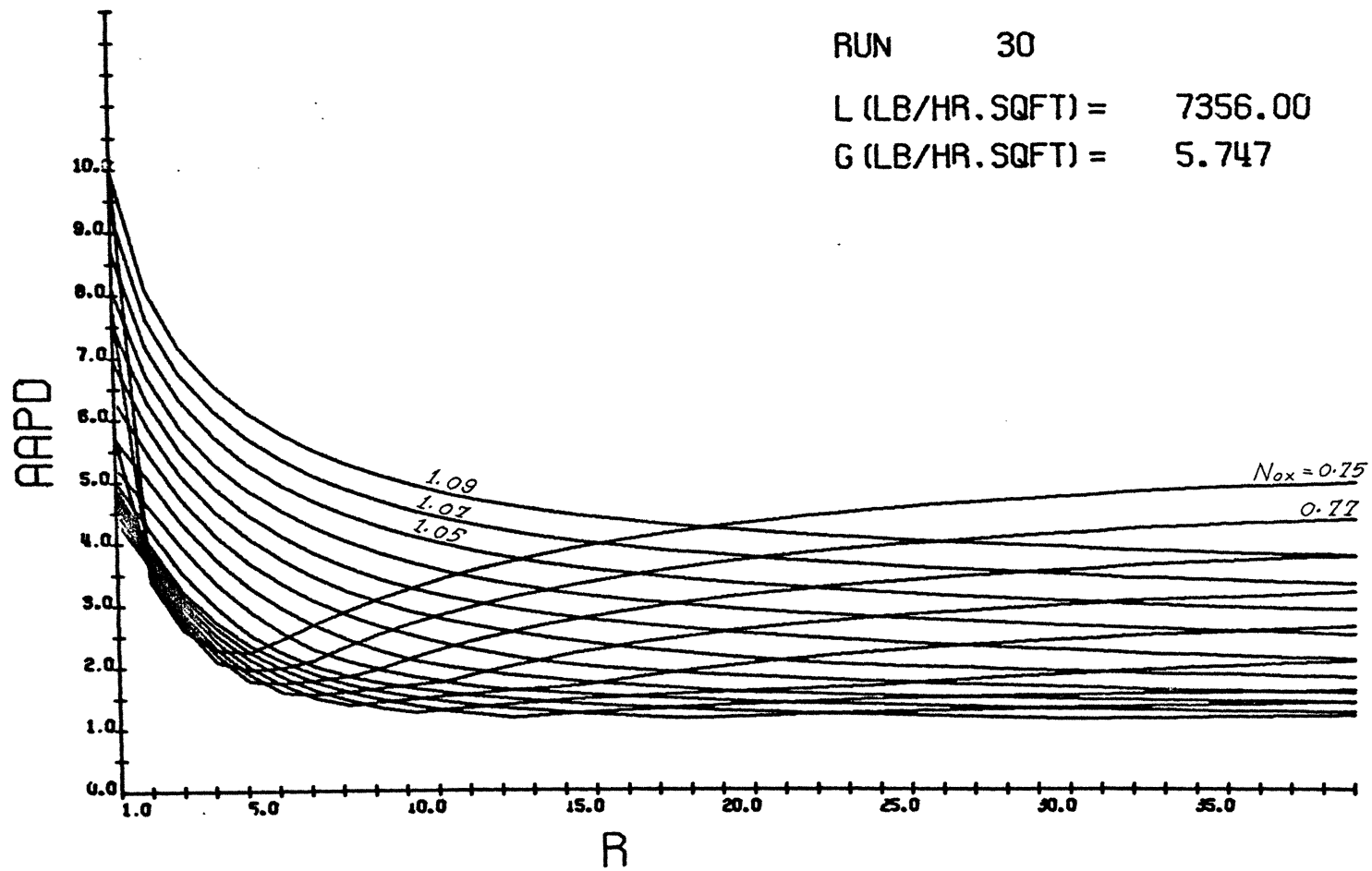


Fig. G-11. Effect of R on AAPD, N_{ox} as the parameter: Run 30. ($L = 7356.00$, $G = 5.747$, $N_{ox} = 0.75$ to 1.09)

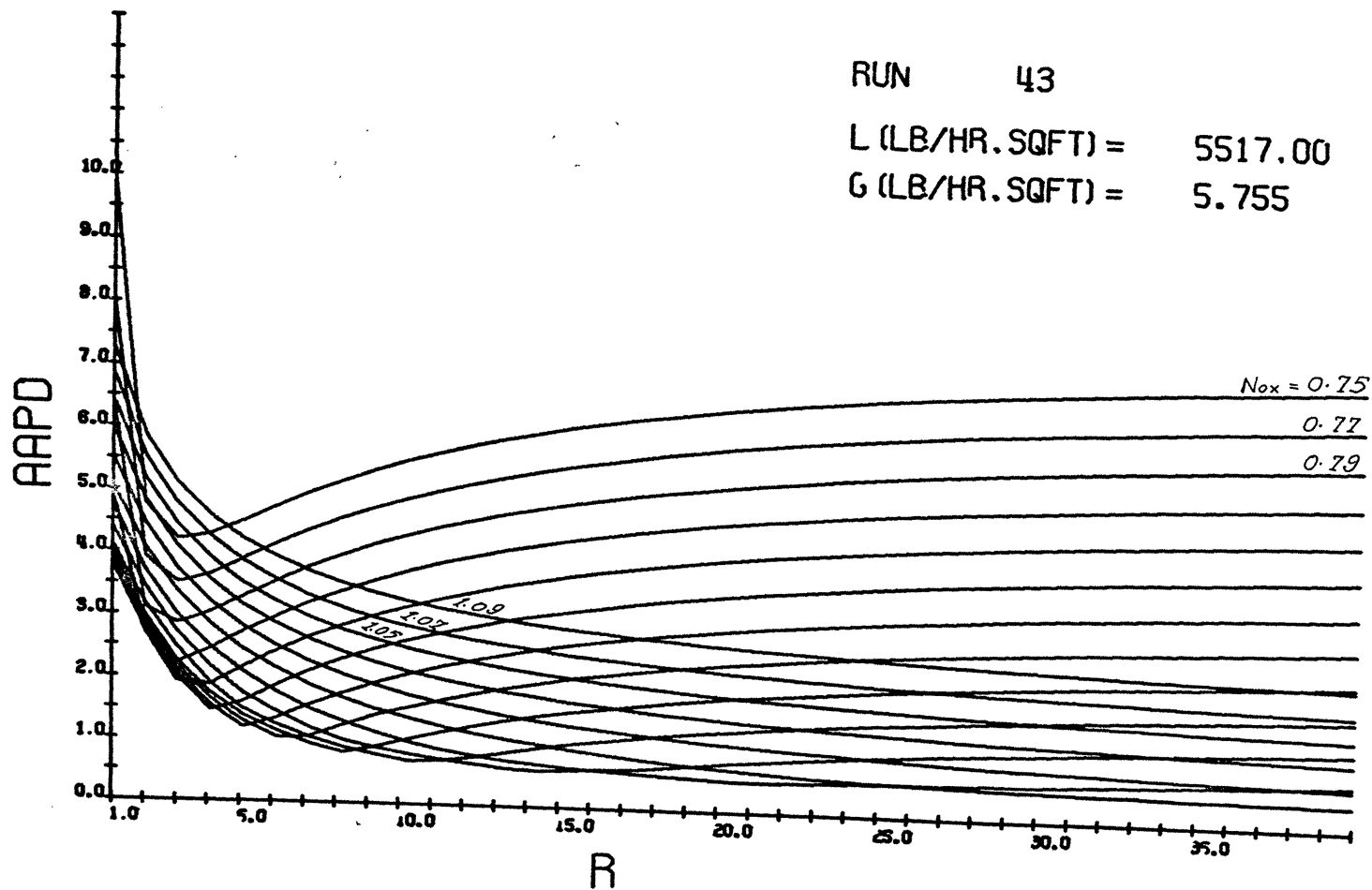


Fig. G -12. Effect of R on AAPD, N_{ox} as the parameter: Run 43. (L = 5517.00, G = 5.755, N_{ox} = 0.75 to 1.09)

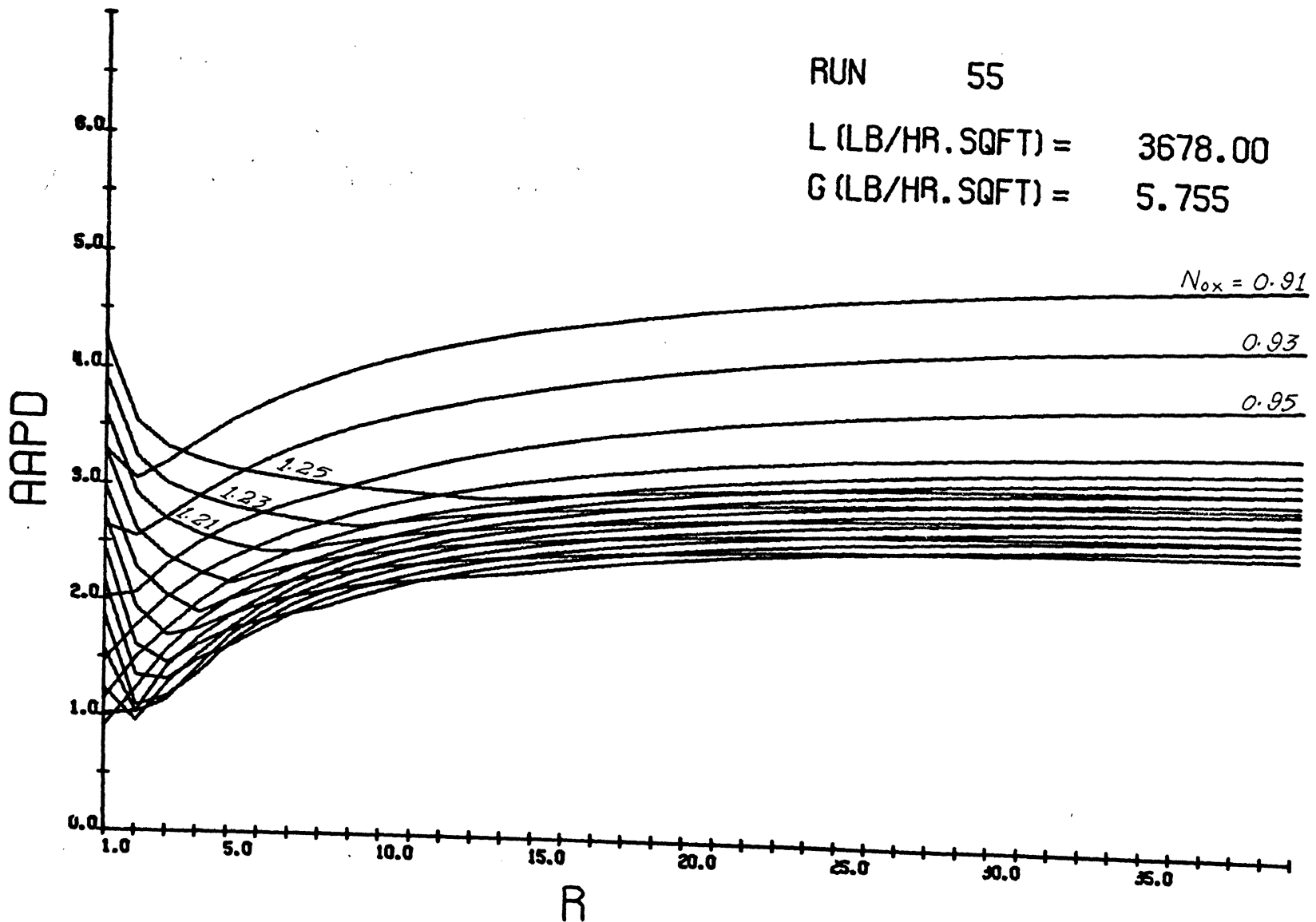


Fig. G-13. Effect of R on AAPD, N_{ox} as the parameter: Run 55. (L = 3678.00, G = 5.755, N_{ox} = 0.91 to 1.25)

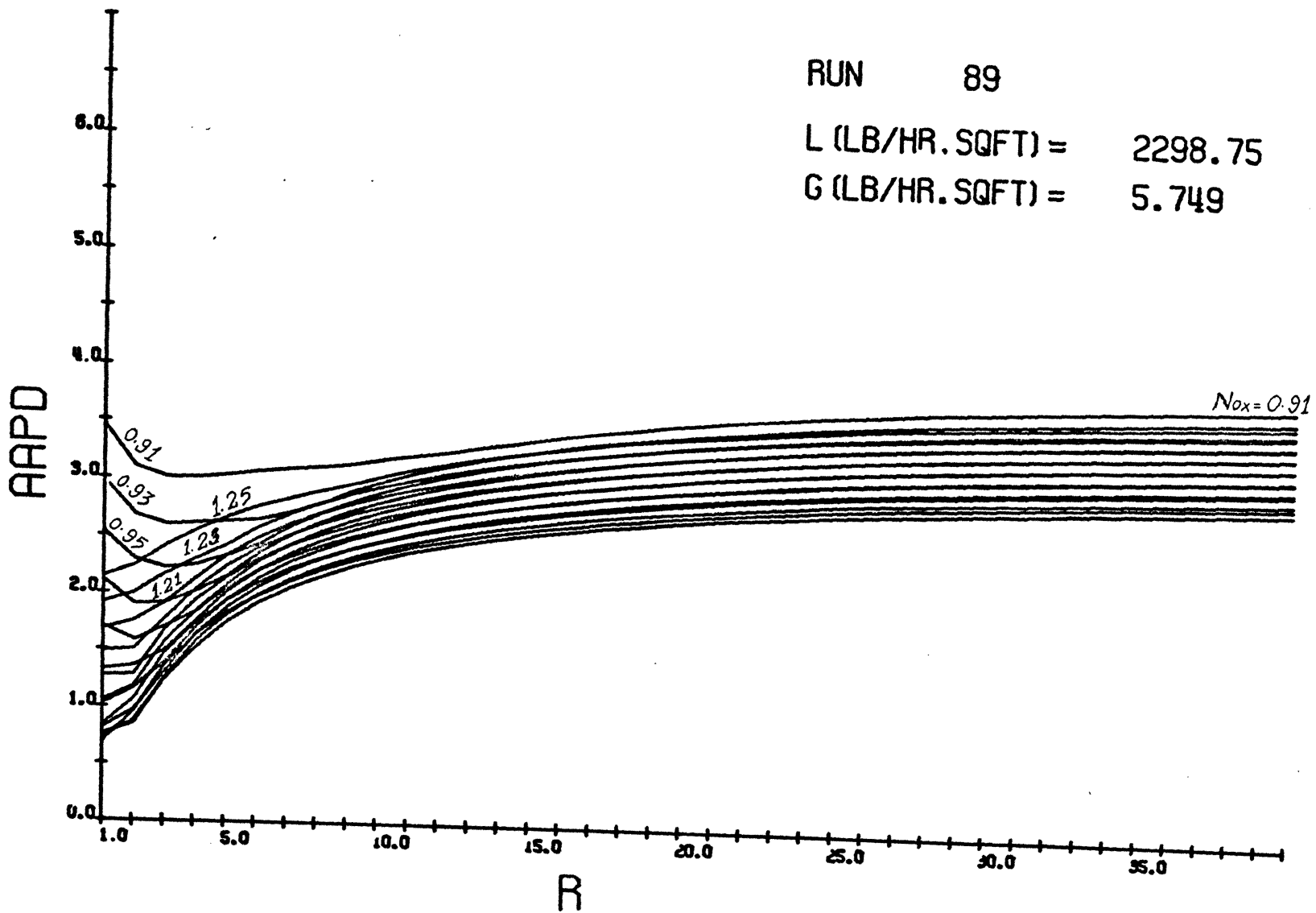


Fig. G-14. Effect of R on AAPD, N_{OX} as the parameter: Run 89. (L = 2298.75, G = 5.749, N_{OX} = 0.91 to 1.25)

RUN 18

L (LB/HR. SQFT) = 9195.00

G (LB/HR. SQFT) = 3.830

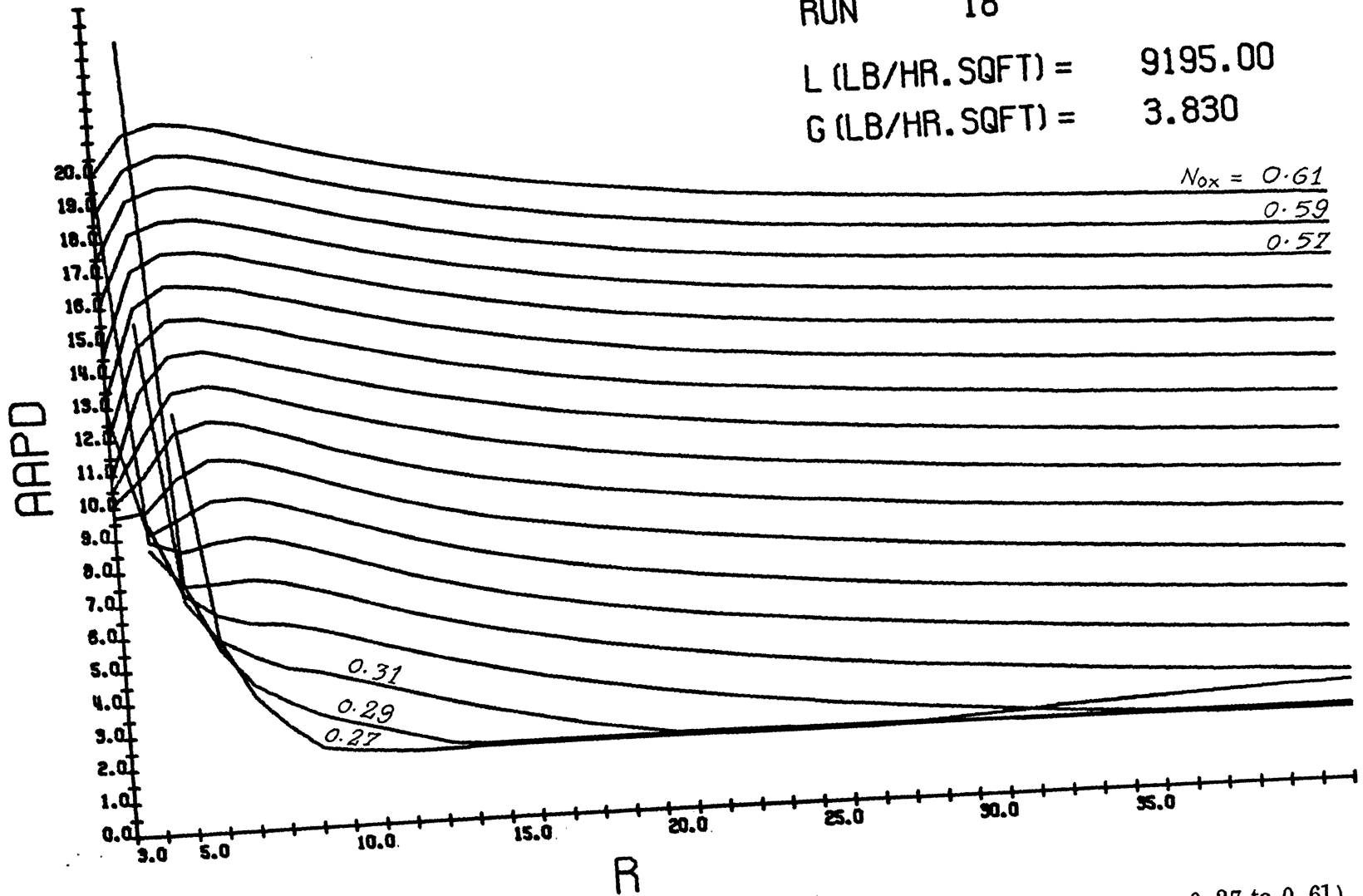


Fig. G-15. Effect of R on AAPD, N_{ox} as the parameter: Run 18. (L = 9195.00, G = 3.830, N_{ox} = 0.27 to 0.61)

RUN 34
 L (LB/HR. SQFT) = 7356.00
 G (LB/HR. SQFT) = 3.822

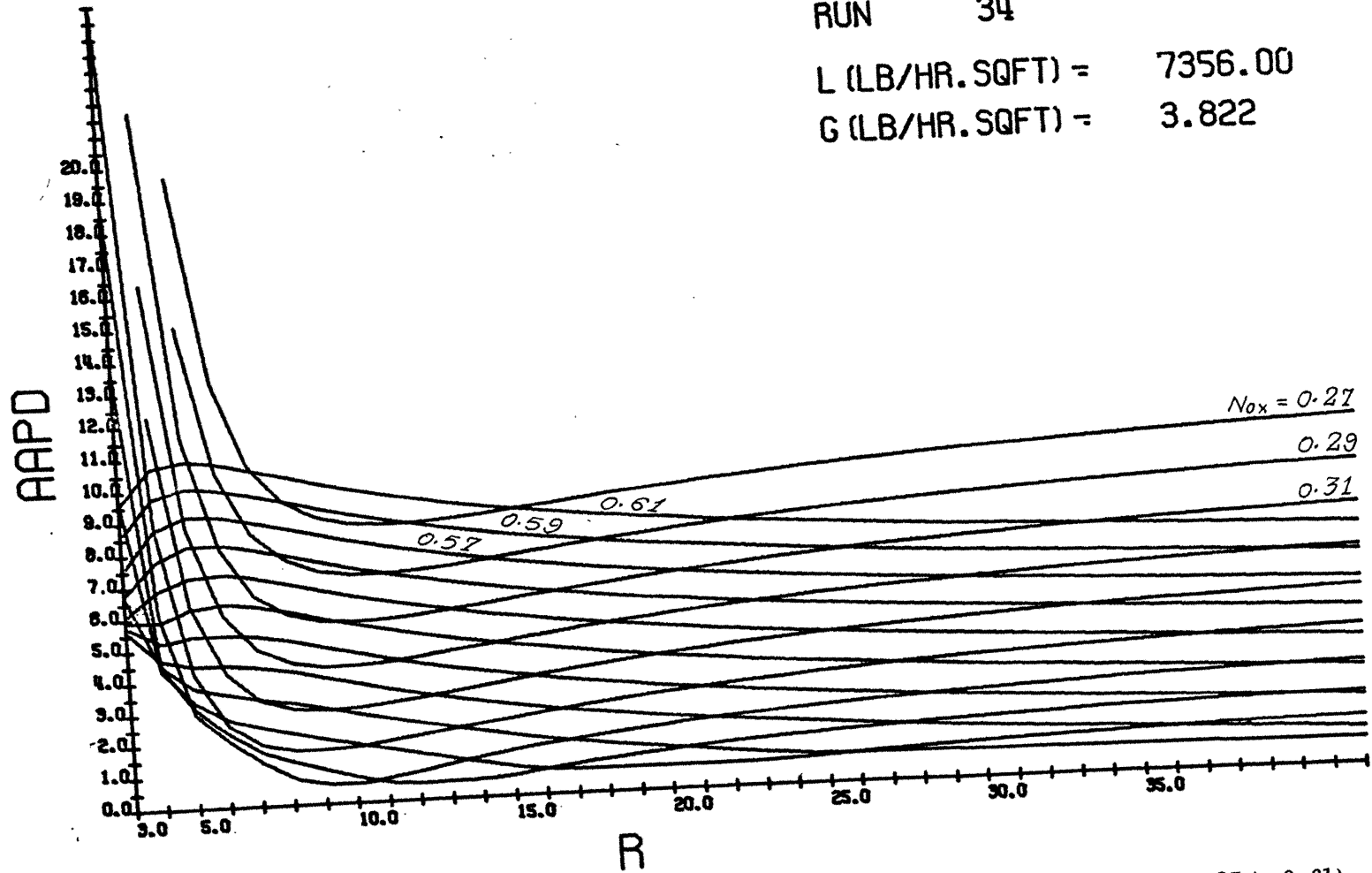


Fig. G-16. Effect of R on AAPD, N_{ox} as the parameter: Run 34. (L = 7356.00, G = 3.822, $N_{ox} = 0.27$ to 0.61)

RUN 45
 L (LB/HR.SQFT) = 5517.00
 G (LB/HR.SQFT) = 3.827

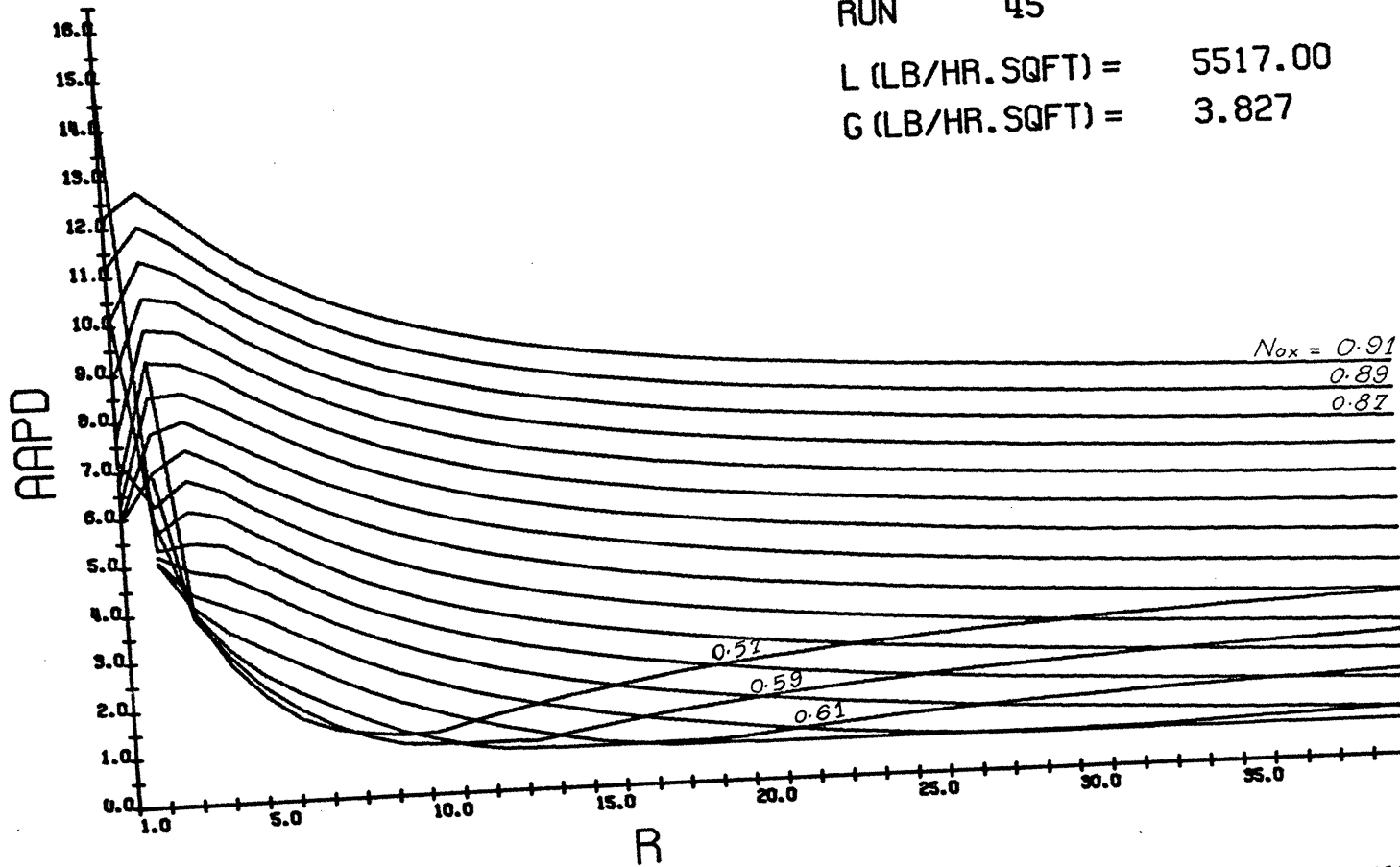


Fig. G-17. Effect of R on AAPD, N_{ox} as the parameter: Run 45. (L = 5517.00, G = 3.827, $N_{ox} = 0.57$ to 0.91)

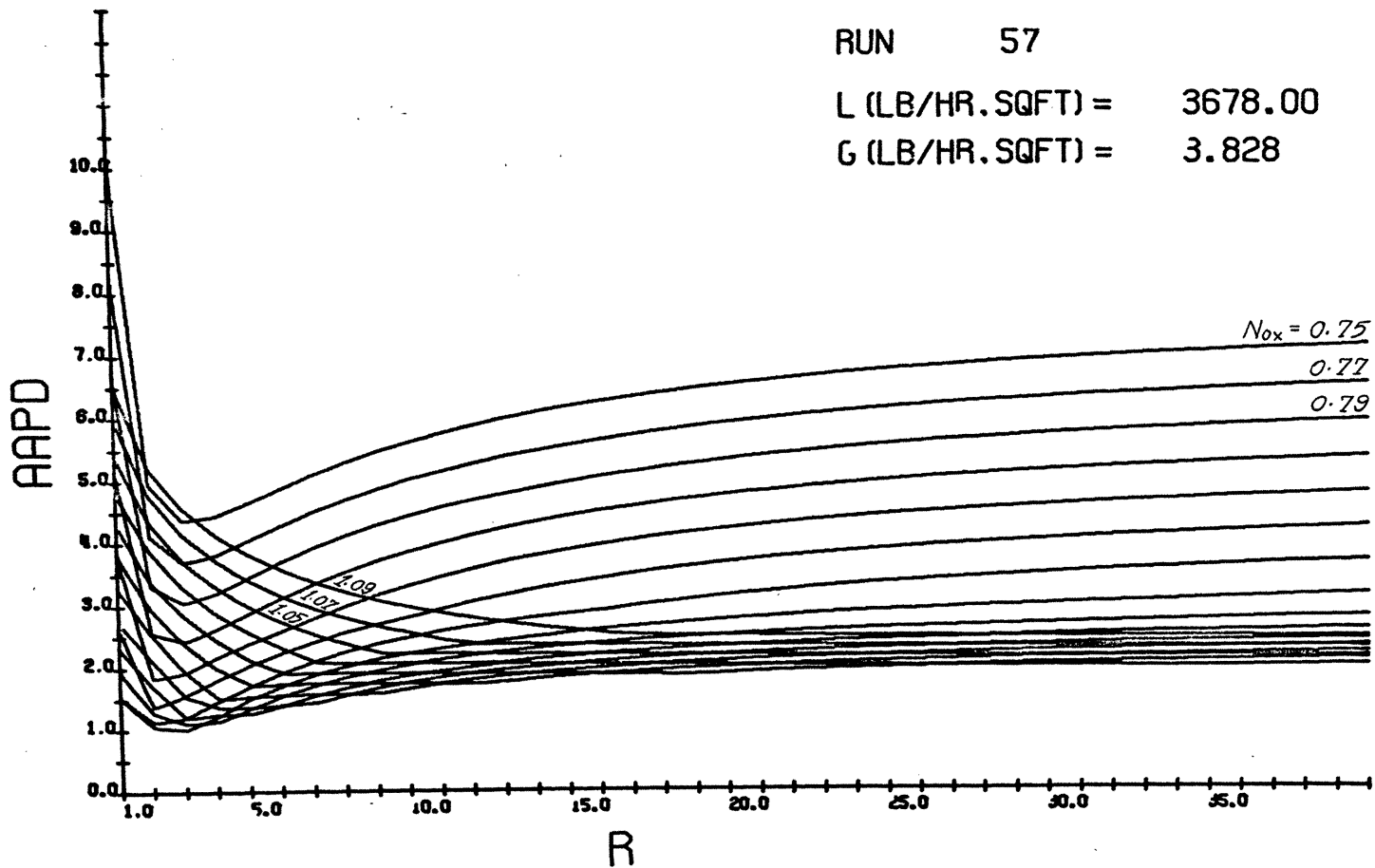


Fig. G-18. Effect of R on AAPD, N_{ox} as the parameter: Run 57. (L = 3678.00, G = 3.828, N_{ox} = 0.75 to 1.09)

VII. BIBLIOGRAPHY

1. Brittan, M.I., M.Sc. Thesis, University Witwatersrand, Johannesburg, South Africa (1964).
2. Brittan, M.I. and E. A. Woodburn, A.I.Ch.E. Journal, 12, 541 (1966).
3. Chilton, T. H. and A. P. Colburn, Ind. Eng. Chem., 27, 255 (1935).
4. Colburn, A. P., Trans. Am. Inst. Chem. Engrs., 29, 174 (1939).
5. Colburn, A. P., Ind. Eng. Chem., 33, 459 (1941).
6. Dankwarts, P. K., Chem. Eng. Sci., 2, 1 (1953).
7. Damkohler, G., "Der Chemie - Ingenieur", A. Eucken and M. Jakob, Akademische Verlagsgesellschaft M.B.H., (Leipzig), 3, pt 1, 366 (1937).
8. Hoffman, H., Chem. Eng. Sci., 14, 193 (1961).
9. Hoftyzen, P. J., "Joint Symposium on Scaling Up", p. 573, Inst. Chem. Engrs., London (1957).
10. Levenspiel, O. and K. B. Bischoff, "Advances in Chemical Engineering", 4, 95, Academic Press, New York (1963).
11. Loomis, A. L., "International Critical Tables", 3, 260, McGraw Hill, New York (1928).
12. McHenry, K. W. and R. H. Wilhelm, A.I.Ch.E. Journal, 3, 83 (1957).
13. Miyauchi, T., "Longitudinal Dispersion in Solvent Extraction Columns", Mathematical Theory, Univ. of Calif. Rad. Lab. Rept., UCRL - 3911, Aug. (1957).
14. Norman, W. S., "Absorption, Distillation and Cooling Towers", pp. 192, 193, Longmans, London (1961).

15. Ogburn, H. , Ph.D. Dissertation, Princeton University, Princeton, New Jersey (1954).
16. Sherwood, T. K. and R. L. Pigford, "Absorption and Extraction", 2nd ed., p. 291, McGraw Hill, New York (1952).
17. Vermeulen, T. and et al, "Longitudinal Dispersion in Packed Extraction Columns", Lawrence Rad. Lab. Rept. , UCRL - 8658, April (1959).
18. Wellek, R. M., Assoc. Prof. of Chem. Engr. , University of Missouri - Rolla, Missouri (1969).

VIII. VITA

The author, Sundareswaran Parameswaran Iyer, was born on January 24, 1944 in Bombay, India. He received his primary and secondary education in Bombay and graduated in 1960. The author received his college education from the University of Bombay. He secured his Bachelor of Chemical Engineering Degree from the Bombay University Department of Chemical Technology, Bombay, in May 1966. From July 1966 to April 1968, the author worked as a Chemical Engineer in a consulting chemical engineering firm in Bombay.

He has been enrolled in the Graduate School of the University of Missouri - Rolla since June 1968, as a candidate for the Master of Science degree in Chemical Engineering.

183304